Editors' choice

The beaver *Steneofiber depereti* from the lower Upper Miocene hominid locality Hammerschmiede and remarks on its ecology

THOMAS LECHNER and MADELAINE BÖHME

Lechner, T. and Böhme, M. 2022. The beaver *Steneofiber depereti* from the lower Upper Miocene hominid locality Hammerschmiede and remarks on its ecology. *Acta Palaeontologica Polonica* 67 (X): xxx–xxx.

Dental remains of a medium sized beaver from the early Late Miocene Hammerschmiede locality (MN 7/8) in the Northern Alpine Foreland Basin (Southern Germany, Bavaria) are described and assigned to *Steneofiber depereti*. The numerous material (160 teeth) was collected in the two fossiliferous layers HAM 5 and HAM 4 and comprises beaver individuals of a large range of age classes, from juvenile to old. The dental remains metrically and morphologically overlap the stratigraphic older *Steneofiber* spp. and the younger *Chalicomys* spp. This supports the hypothesis of the European anagenetic evolutionary lineage *Steneofiber depereti–Chalicomys jaegeri*. The morphological characters to differentiate *Steneofiber depereti* and *Chalicomys jaegeri* are discussed and redefined. The performed age-frequency distribution (Mortality profile) indicates a natural ecological mortality and confirms that at least the fluvial channel of the HAM 4 deposits was the actual optimal beaver habitat and continuously populated by larger family groups of beavers. Furthermore, there are indications that the Hammerschmiede beaver had a similar parental investment as today's beavers, where young adults migrate to poorer habitats in the second year, in search of their own territory. The shallower channel of HAM 5 possibly represents such a "second choice" habitat.

Key words: Mammalia, Rodentia, Castoridae, *Steneofiber depereti*, ecology, mortality, Miocene, Germany, Bavaria.

Thomas Lechner [thomas.lechner@senckenberg.de] and Madelaine Böhme [m.boehme@ifg.uni-tuebingen.de], Senckenberg Centre for Human Evolution and Paleoenvironment (HEP), Eberhard Karls University of Tübingen, Institute for Geoscience, Sigwartstraße 10, 72074 Tübingen, Germany.

Received 22 march 2022, accepted 16 June 2022, available online 23 November 2022.

Introduction

The early Late Miocene Hammerschmiede locality (Allgäu region, Bavaria) is long known for its rich vertebrate fauna (Fahlbusch and Mayr 1975; Mayr and Fahlbusch 1975). Since the early 2000s, excavations by the University of Tübingen yielded approximately 20 000 new specimens. Currently, the vertebrate fauna of the Hammerschmiede locality comprises more than 130 vertebrate taxa (Kirscher et al. 2016; Böhme et al. 2019). Since the description of the arboreal biped hominid *Danuvius guggenmosi* Böhme, Spassov, Fuss, Tröscher, Deane, Prieto, Kirscher, Lechner, and Begun, 2019, the Hammerschmiede locality became internationally renowned (Böhme et al. 2020; Williams et al. 2020). Apart from this exceptional finding, other groups of the vertebrate fauna of the Hammerschmiede have been published, including the antelope *Miotragocerus monacensis* Stromer von Reichenbach, 1928 (Fuss et al. 2015; Hartung et al. 2020), the mouse deer *Dorcatherium naui* Kaup, 1833 (Hartung and Böhme 2022), birds including a large crane, the darter *Anhinga pannonica* Lambrecht, 1916, and anseriforms represented by the small cf. *Mioquerquedula* sp. and the new anatid *Allgoviachen tortonica* Mayr, Lechner, and Böhme, 2022 (Mayr et al. 2020a, b, 2022), carnivores (Kargopoulos et al. 2021a–c, 2022) and small mammals including soricids, erinaceids, eomyids and cricetids (Prieto and Rummel 2009; Prieto et al. 2011; Prieto 2012; Prieto and Dam 2012). Turtles, artiodactyles, carnivores, fishes, and rodents are the most common vertebrates in the Hammerschmiede fauna, indicating a diverse ecosystem consisting of arboreal, terrestrial, semiaquatic and aquatic habitats. One of the most common groups of semiaquatic vertebrates are the beavers (Castoridae) that are represented by numerous specimens.

Today, beavers are solely represented by the genus *Castor*, but during the European Miocene a much higher diversity of up to seven genera are known, *Anchitheriomys* Roger, 1898, *Chalicomys* Kaup, 1832, *Dipoides* Jaeger, 1835, *Eucastor*? (*Schreuderia*) Aldana Carrasco, 1992, *Euroxenomys* Samson

and Radulesco, 1973, *Steneofiber* Geoffroy-Saint-Hilare, 1833 and *Trogontherium* Fischer von Waldheim, 1809 (Hugueney 1999; Stefen 2009). All these beavers are usually interpreted to inhabit similar ecological niches. Therefore, it is not surprising that in most localities that contain fossil beavers, only a single beaver species is known (Rekovets et al. 2020). But there are several localities with two beaver taxa (Hugueney 1999; Rekovets et al. 2020) including: Hambach (MN 5; Stefen and Mörs 2008; Mörs and Stefen 2010) with the equal-sized *Steneofiber depereti* Mayet, 1908, and *Anchitheriomys suevicus* Schlosser, 1884, as well as other localities with beaver taxa that have a notable size difference including: Dorn-Dürkheim 1 (MN 11; Franzen and Storch 1975; Rekovets et al. 2009, 2020; Casanovas-Vilar and Alba 2011) and Grytsiv (MN 9; Rekovets et al. 2020) with *Chalicomys jaegeri* (= *C. plassi*) Kaup, 1832, and *Euroxenomys minutus* (Von Meyer, 1838), and Sansan (MN 6; Hugueney and Duranthon 2012) with *Steneofiber* aff. *eseri* (Von Meyer, 1846) and *Euroxenomys minutus*. Only few localities comprise more than two beaver taxa, including Staniantsi (MN 13; Lechner and Böhme 2020) with *Castor sp*. Linnaeus, 1758, *Dipoides problematicus* Schlosser, 1902 and *Euroxenomys minutus*. At the locality Hammerschmiede two different beavers, the medium sized *Steneofiber depereti* and the small *Euroxenomys minutus* are found, though previous publications assigned the incisor fragment of a medium sized beaver from Hammerschmiede to *Chalicomys jaegeri* (Mayr and Fahlbusch 1975; Hugueney 1999; Kirscher et al. 2016: table 1; Böhme et al. 2019: supplementary table S1).

In this study we report new dental material of the larger castorid from Hammerschmiede (consisting of 142 specimens including 160 teeth). Based on diagnostic features we assign this material to *Steneofiber depereti*. The exceptionally high number of specimens with different age stages, provides insights into the intraspecific and ontogenetic variability of the *Steneofiber* population. The presence of beavers in Hammerschmiede is indicative for a freshwater dominated river ecosystem. This interpretation is also supported by the sediments of the Hammerschmiede clay pit (Fuss et al. 2015; Kirscher et al. 2016).

Institutional abbreviations.—GPIT, University of Tübingen, Germany; SNSB-BSPG, Bavarian State Collection of Palaeontology and Geology, Munich, Germany.

Other abbreviations.—D/d, upper/lower deciduous teeth; HAM, Hammerschmiede layers (HAM 5 and HAM 4); I/i, upper/lower incisor; M/m, upper/lower molar; M1/2 or m1/2, upper or lower first or second molar, more precise differentiation of the tooth position not possible; P/p, upper/lower premolar; WS 1–6, dental wear stages.

Geological setting

The locality Hammerschmiede is situated close to the small town Pforzen, only a few kilometres northwest of Kaufbeuren (Bavaria, Southern Germany) in the Northern Alpine Foreland Basin. The active clay pit (clay, silty-clay and fine-sand) comprises a 26-metre-thick sediment section mainly represented by floodplain and channel deposits from the early Late Miocene age (Tortonian, MN 7/8). Within this section there are two main fossiliferous layers, HAM 5 and HAM 4 with an approximate depositional age of 11.62 and 11.44 Ma, respectively (Kirscher et al. 2016). The younger HAM 4 horizon can be interpreted as a river channel of about 50 m width and 4–5 m depth (Mayr et al. 2020a) whereas the slightly older HAM 5 most likely represents a small rivulet of only four to five metres width (Mayr et al. 2020a). According to the classic stream order (Hack's stream order following Hack 1957) it is assumed, that HAM 4 represents a deeper 2nd order stream and HAM 5 a shallower 3rd order stream.

Material and methods

The material used in this study was excavated at the Hammerschmiede locality. In total 160 teeth (142 specimens) were examined, of which 42 (39 specimens) are from the HAM 5 layer and 118 (103 specimens) from the HAM 4 layer.

The entire material is stored in the palaeontological collection of the University of Tübingen, Germany (GPIT), and is labelled either with GPIT (for excavation years 2011 to 2019 inclusive) or SNSB-BSPG (Bavarian State Collection of Palaeontology and Geology in Munich, Germany; for excavation years 2020 to 2021). SNSB-BSPG 2020 XCIV identifies specimens from HAM 4 and SNSB-BSPG 2020 XCV from HAM 5.

The morphological nomenclature of dental material follows Stirton (1935) and Hugueney (1999) (Fig. 1). The nomenclature of skull and mandibular features follows Freye (1959). Dental measurements were taken with a digital calliper (rounded to the first decimal point) at the occlusal surface and at the position of maximum extent (basal tooth) when possible. Evaluation of dental wear stages (WS) is modified according to Stefen (1997, 2001, 2018), Stefen and Mörs (2008), and Heinrich and Maul (2020): WS 1, unworn: no wear can be observed, deciduous dentition in use; WS 2, slightly worn: first occlusal contact; WS 3, worn: para-/metaflexus/-id is closing or just closed; WS 4, medium worn: mesoflexus/-id is closing or just closed; WS 5, deeply worn: hypoflexus/-id is near to closing; WS 6, heavily worn: hypoflexus/-id is closed.

Systematic palaeontology

Class Mammalia Linnaeus, 1758
Order Rodentia Bowdich, 1821
Family Castoridae Hemprich, 1820
Subfamily Castorinae Hemprich, 1820

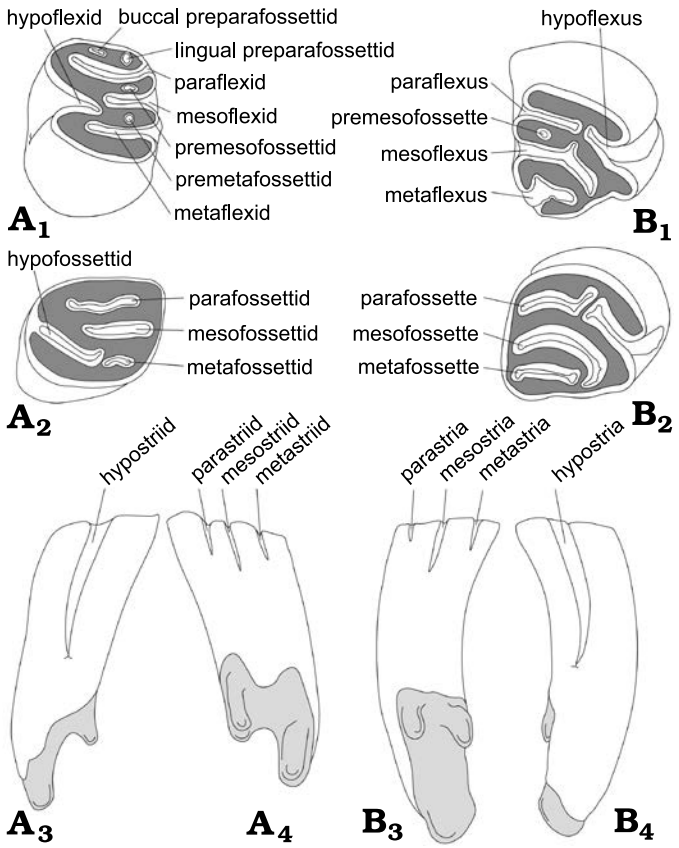

Fig. 1. General tooth scheme and morphological nomenclature used for the descriptions and comparisons of right lower (**A**) and upper (**B**) cheek teeth (premolars and molars) of the beaver *Steneofiber depereti* Mayet, 1908, from the early Late Miocene locality of Hammerschmiede (Bavaria, Germany). A_1, B_1, occlusal view of an early wear stage; A_2, B_2,occlusal view of a later wear stage; A_3, B_3, buccal view; A_4, B_4, lingual view. Enamel in white, dentine in dark grey, roots in light grey, cement not shown. Line drawings are not based on specific specimens and are not to scale. Nomenclature follows Stirton (1935) and Hugueney (1999).

Genus *Steneofiber* Geoffroy-Saint-Hilaire, 1833

Type species: *Steneofiber eseri* (*Chalicomys eseri* Meyer, 1846 = *Steneofiber castorinus* Pomel, 1847). Following Hugueney 1999, the genus *Steneofiber* "published before 1931 ...(as) uninominal genus group named without associated nominal species is accepted as consistent with the Principles of Binomial Nomenclature in the absence of evidence to the contrary" (ICZN, art 11 c, i). Saint-Gérant-le-Puy (France), Early Miocene (MN 2).

Steneofiber depereti Mayet, 1908

Figs. 2–6.

For synonymy see Hugueney (1999).

Material.—Hammerschmiede locality, Germany, lower Upper Miocene, MN 7/8, base of Tortonian, for measurements see Tables 1 and 2). *HAM 5, upper dentition*: left I2: GPIT/MA/10749; right I2: GPIT/MA/10753; left DP4: GPIT/MA/10744, 10781; left P4: GPIT/MA/10746; left M1/2: GPIT/MA/10731, 13820; right M1/2: GPIT/MA/12604, 13825; left M3: GPIT/MA/10748, 12152. *HAM 5, lower dentition:* left i2: GPIT/MA/10743; right i2: GPIT/MA/10729; left dp4: GPIT/MA/10782; right dp4: GPIT/MA/10785, 13826; left p4: GPIT/MA/09896, 10727, 13980, SNSB-BSPG 2020 XCV-0303; right p4: GPIT/MA/10745; left m1/2: GPIT/MA/09897, 09902, 09906, 10728, 10784, 12342, 13822, 13824; right m1/2: GPIT/MA/09903, 12032, 12260, 13821; right m3: GPIT/MA/09907, 10751, 13823; right mandible with angular process, part of the coronoid process, i2 and m1: GPIT/MA/13813; right mandible with angular process, p4, m1 and m3: GPIT/MA/09909; right mandible (frag.) with i2: GPIT/MA/10742. *HAM 4, upper dentition*: right I2: GPIT/MA/17456, 17807, SNSB-BSPG 2020 XCIV-0661; left DP4: GPIT/MA/12416, 12489; right DP4: GPIT/MA/17763, SNSB-BSPG 2020 XCIV-0879, 1731; left P4: GPIT/MA/17205, 10989, SNSB-BSPG 2020 XCIV-1725, 3891, 5375; right P4: GPIT/MA/17422, 17772, 16935, 17081, SNSB-BSPG 2020 XCIV-1510; left M1/2: GPIT/MA/16755, 12490, 16134, SNSB-BSPG 2020 XCIV-1724, 5366, 5371; right M1/2: GPIT/MA/17358, 16845, SNSB-BSPG 2020 XCIV-1391, 1726, 1727, 4059, 5367, 5368, 5369, 5370, 5372, 5374, 5376, 5377, 5378; left M3: GPIT/MA/12562, 16530, SNSB-BSPG 2020 XCIV-0415, 1320, 1728, 1729; right M3: GPIT/MA/10990, SNSB-BSPG 2020 XCIV-0446, 1730, 3388, 5373; maxillae and palatine (frag.) with left P4–M1 and right P4: GPIT/MA/17163; right P4–M2 (frag.): GPIT/MA/17367; left maxilla (frag.) with P4: GPIT/MA/16979.

Table 1. Dimensions (in mm) of upper and lower teeth of the beaver *Steneofiber depereti* Mayet, 1908, from the lower Upper Miocene locality of Hammerschmiede (Bavaria, Germany), with combined treatment of material from the local stratigraphic levels HAM 5 and HAM 4. L, mesio-distal length at occlusal surface and at basal position (where possible) for cheek teeth and length across anterior enamel band for incisors; W, bucco-lingual width at occlusal surface and at basal position (where possible) for cheek teeth; m, measurement; N, number of measurements.

Tooth position	m	N	Min	Max	Mean	Standard deviation	Variance
i	L	11	4.14	7.92	6.43	1.28	1.64
	W	11	4.15	7.47	6.01	1.28	1.64
I	L	4	5.77	7.06	6.54	0.56	0.32
	W	5	5.85	7.42	6.56	0.61	0.37
dp4	L	8	6.56	8.26	7.26	0.61	0.38
	W	8	4.52	5.66	5.13	0.39	0.15
p4	L	29	6.47	12.34	10.07	1.31	1.71
	W	29	5.98	8.23	7.34	0.53	0.28
m1/2	L	71	5.74	8.02	6.56	0.48	0.23
	W	71	4.55	8.37	6.89	0.89	0.80
m3	L	26	5.78	7.77	6.60	0.49	0.24
	W	26	5.17	7.05	6.31	0.39	0.15
DP4	L	10	5.00	6.80	5.94	0.63	0.40
	W	13	4.19	9.82	6.71	1.62	2.63
P4	L	34	7.59	9.56	8.21	0.53	0.28
	W	34	7.39	9.84	8.72	0.59	0.35
M1/2	L	52	4.98	7.40	5.89	0.46	0.21
	W	52	4.06	7.97	6.65	0.91	0.83
M3	L	24	5.16	6.41	5.82	0.33	0.11
	W	24	3.97	7.00	5.93	0.78	0.61

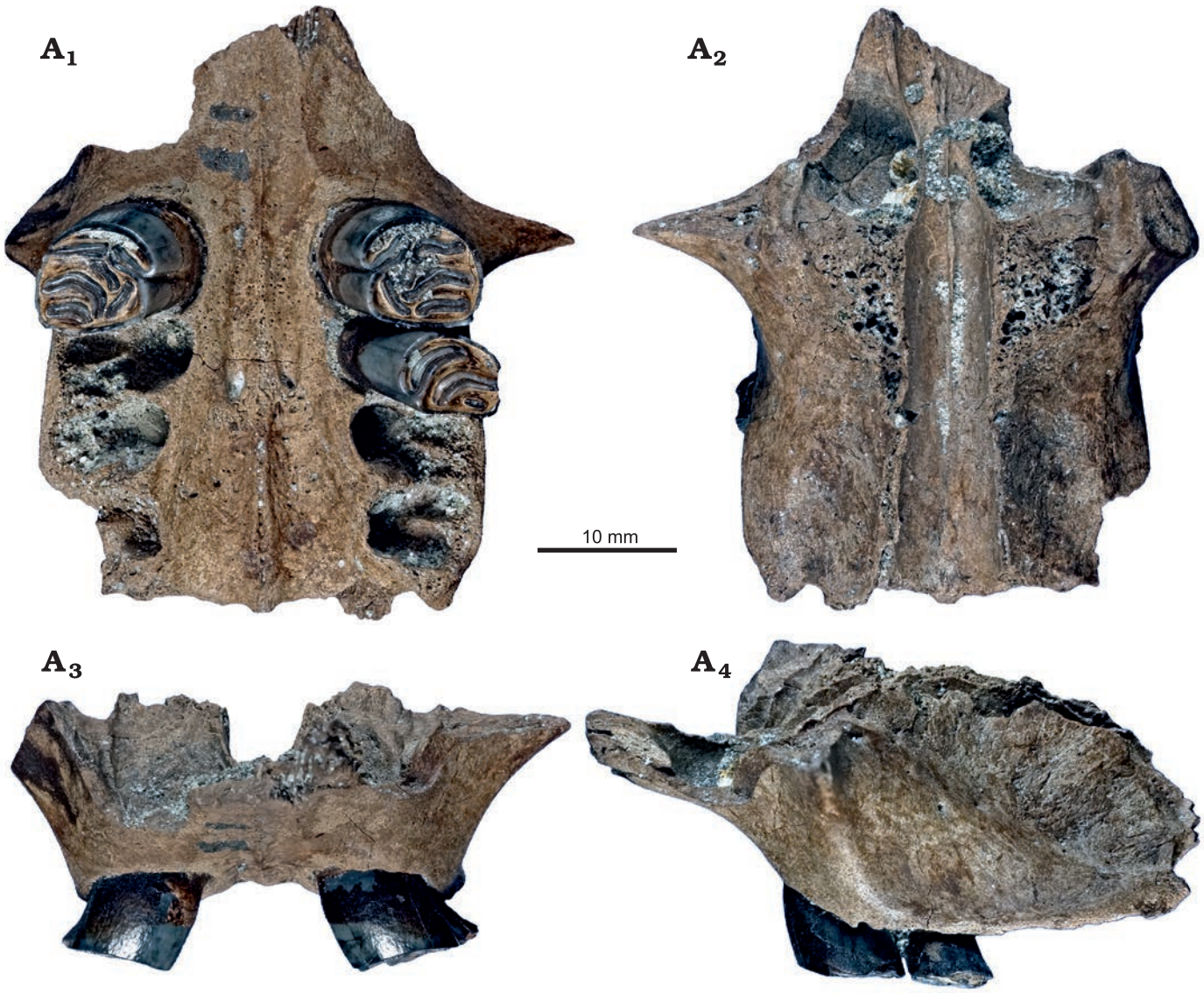

Fig. 2. Maxillae and fragmentary palatine of the beaver *Steneofiber depereti* Mayet, 1908 (GPIT/MA/17163), from the early Late Miocene locality Hammerschmiede (Bavaria, Germany), local stratigraphic level HAM 4. Maxillae and fragmentary palatine with left P4–M1 and right P4 in occlusal (A_1), dorsal (A_2), mesial (A_3), and left buccal (A_4) views.

HAM 4, lower dentition: left i2: GPIT/MA/16985, SNSB-BSPG 2020 XCIV-1100; right i2: GPIT/MA/16512, 16928, 16436; left dp4: SNSB-BSPG 2020 XCIV-5365; left p4: GPIT/MA/17296, 17352, SNSB-BSPG 2020 XCIV-0179, 0487, 1246, 3726; right p4: GPIT/MA/18113, SNSB-BSPG 2020 XCIV-2276, 5362; left m1/2: GPIT/MA/16908, SNSB-BSPG 2020 XCIV-3572, 3745, 5359, 5363, 5364; right m1/2: GPIT/MA/10987, 16672, 16915, SNSB-BSPG 2020 XCIV-1185, 1468, 1723, 3903, 5357, 5358, 5360; left m3: GPIT/MA/17388, SNSB-BSPG 2020 XCIV-0416, 1114, 1719, 5361; right m3: GPIT/MA/17666, SNSB-BSPG 2020 XCIV-1720, 1721, 1722; left mandible with i2, dp4, m1, m2 (juvenile): GPIT/MA/17569; left mandible with dp4, m1, m2, m3 (juvenile): GPIT/MA/16950; left mandible with i2 (frag.), p4 (frag.), m1, m2: GPIT/MA/17068; left mandible with p4, m1, m2: SNSB-BSPG 2020 XCIV-1494; right mandible with p4 (frag.), m1, m2: GPIT/MA/16839; right mandible (frag.) with m2, m3: GPIT/MA/17280; left mandible (frag) with m1: GPIT/MA/18106; right mandible (frag.) with m2: SNSB-BSPG 2020 XCIV-2134; left angular process: GPIT/MA/16586; right angular process: GPIT/MA/17215.

Description.—In general, all cheek teeth are subhypsodont to hypsodont, developing complete and closed roots with age. Hypostriid and hypostria are always the longest striid/stria, but they never extend to the crown base although they can get quite close to it in the lower premolars. Mesostriid/-ia are usually longer than para- and metastriid/-stria, with the latter always terminating within the first quarter of tooth crown. The premolar is the largest tooth of the cheek teeth. Flexus/-ids, fossettes/-ids and striae/striids are gradually filled with cement with increasing wear stages and age.

Upper dentition: GPIT/MA/17163 is the most complete specimen with parts of the maxillae and palatine including

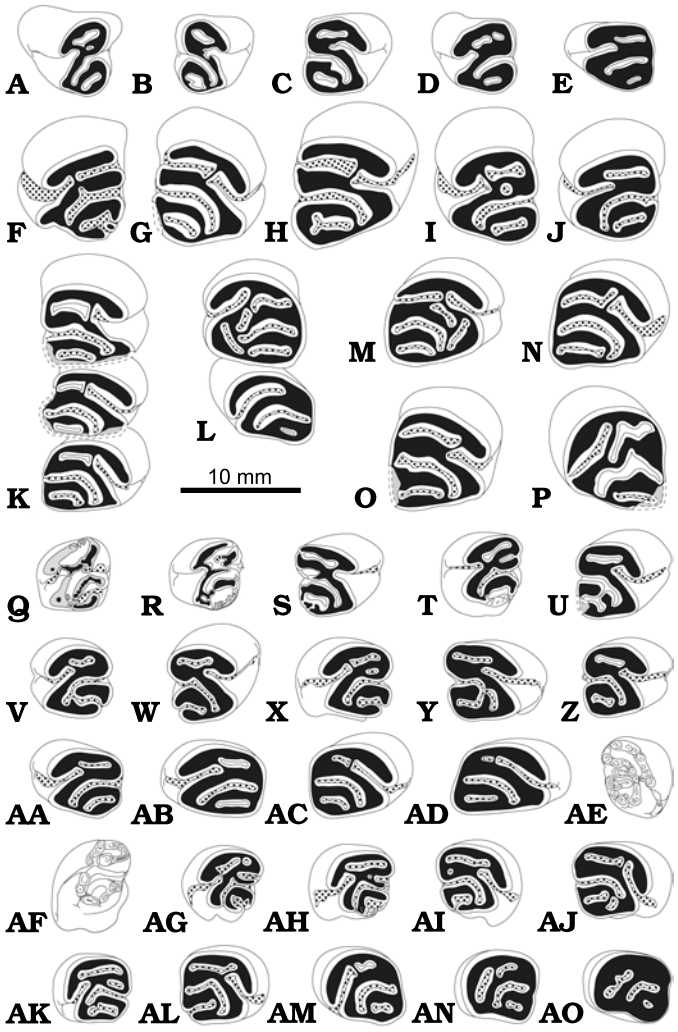

Fig. 3. Occlusal pattern of upper cheek teeth of the beaver *Steneofiber depereti* Mayet, 1908, from the early Late Miocene locality Hammerschmiede (Bavaria, Germany), local stratigraphic levels HAM 5 and HAM 4. Deciduous premolars (**A**–**E**), premolars (**F**–**J**, **M**–**P**), maxillary tooth rows (**K**, **L**), molars(**Q**–**AQ**). Left DP4: (**A**) GPIT/MA/12416, HAM 4; (**D**) GPIT/MA/10744, HAM 5; (**E**) GPIT/MA/10781, HAM 5. Right DP4: (**B**) SNSB-BSPG XCIV-0879, HAM 4; (**C**) GPIT/MA/17763, HAM 4. Left P4: (**F**) SNSB-BSPG XCIV-3891, HAM 4; (**I**) SNSB-BSPG XCIV-5375, HAM 4; (**J**) GPIT/MA/10989, HAM 4; (**P**) GPIT/MA/10746, HAM 5. Right P4: (**G**) GPIT/MA/17422, HAM 4; (**H**) GPIT/MA/17772, HAM 4; (**M**) GPIT/MA/17163, HAM 4; (**N**) GPIT/MA/16935, HAM 4; (**O**) GPIT/MA/17081, HAM 4. Right P4–M2: (**K**) GPIT/MA/17367, HAM 4. Left P4–M1: (**L**) GPIT/MA/17163, HAM 4. Left M1/2: (**Q**) SNSB-BSPG XCIV-5366, HAM 4; (**R**) GPIT/MA/13820, HAM 5; (**T**) SNSB-BSPG XCIV-5371, HAM 4; (**S**) SNSB-BSPG XCIV-5372, HAM 4; (**V**) GPIT/MA/16134, HAM 4; (**X**) SNSB-BSPG XCIV-1724, HAM 4; (**AA**) GPIT/MA/12490, HAM 4; (**AB**) GPIT/MA/16755, HAM 4. Right M1/2: (**U**) SNSB-BSPG XCIV-1391, HAM 4; (**W**) GPIT/MA/16845, HAM 4; (**Y**) SNSB-BSPG XCIV-5370, HAM 4; (**Z**) SNSB-BSPG XCIV-5368, HAM 4; (**AC**) GPIT/MA/17358, HAM 4; (**AD**) SNSB-BSPG XCIV-1726, HAM 4. Right M3: (**AE**) SNSB-BSPG XCIV-3388, HAM 4; (**AI**) GPIT/MA/10990, HAM 4; (**AJ**) SNSB-BSPG XCIV-5373, HAM 4; (**AL**) SNSB-BSPG XCIV-0446, HAM 4. Left M3: (**AF**) SNSB-BSPG XCIV-1320, HAM 4; (**AG**) SNSB-BSPG XCIV-0415, HAM 4; (**AH**) GPIT/MA/12562, HAM 4; (**AK**) GPIT/MA/10748, HAM 5; (**AM**) GPIT/MA/16530, HAM 4; (**AN**) SNSB-BSPG XCIV-1728, HAM 4; (**AO**) SNSB-BSPG XCIV-1729, HAM 4. Enamel in white, dentine in black, cement as dotted area, completions or hypothetic area of first wear in grey.

both P4, the left M1 and the alveoli of all other molars. Another maxilla fragment (GPIT/MA/16979) consists of a left P4 (Fig. 2). GPIT/MA/17367 comprises a right P4, M1 and M2; however, the remains of the maxilla were too weathered to be rescued. The rest of the material of the upper dentition is represented by isolated teeth; in total, five I2 fragments, seven DP4, 15 P4 (three in situ), 28 M1/2 (three in situ) and 13 M3.

I2: Five upper incisor fragments were excavated, all with their tips preserved. Their wear facets are all terraced and divided into two different parts. The labial tooth surface shows a smooth enamel band. A sharp and steep anterior tip consisting of mostly the labial enamel band and the angled lingual part of the dentine shows small and irregularly stepped wear marks parallel to the enamel band. The cross section of the upper incisor depicts an equilateral triangle with slightly convex sides (Reuleaux triangle). The lingual tip of this triangle is directed mesially.

DP4: All seven DP4 are worn and their para- and metafossettes are clearly visible (Figs. 3A–E, 4A, B), but only in four specimens an open mesoflexus is exposed (Figs. 3A–D, 4A, B). GPIT/MA/10781 is the most worn DP4 and its mesoflexus is closing (Fig. 3E). In all DP4 the hypoflexus/-stria are still open and do not reach the base of the crown (Figs. 3A–E, 4A, B_1). Two DP4 show an additional small fossette, one laterally to the parafossette (GPIT/MA/10744; Figs. 3D, 4A) and one between parafossette and mesoflexus (GPIT/MA/12416; Fig. 3A). Synclines of DP4 are never filled with cement. Only two DP4 have their entire base preserved (GPIT/MA/10744 and 17763) that consists of three roots with two small uniform buccal roots and one large dominant lingual root (Fig. $4B_1$, B_2).

P4: In general, the occlusal surface of the P4 is nearly as wide as long (Figs. 3F–P, 4C–F). Mesiolingually the P4 is rounded, whereas the posterior and buccal margins are straight, forming an angular edge. The hypostria always closes well above the tooth base (Fig. $4D_2$, E_2, F). Striae, flexus and fossettes of all P4 are at least slightly filled with cement in the least worn specimens (SNSB-BSPG 2020 XCIV-1510 and 3891; Figs. 3F, 4C) and cement filling increases with wear and age. The P4 is double-rooted with one minor root located at the distobuccal edge (Fig. $4D_3$). The dominant root forms a wide arch that follows the mesiolingual tooth margin. The least worn P4 (SNSB-BSPG 2020 XCIV-1510) is the only unrooted P4 consisting of the tooth crown solely.

Only in the least worn SNSB-BSPG 2020 XCIV-3891 a metaflexid and a tiny enamel stylid at the buccal margin are expressed, but near to closure (Figs. 3G, 4C). All other available P4 are worn and the metafossette is exposed (Fig. 3G–P). Their para- and mesostria are very short or in higher wear stages they are already closed as fossettes (Figs. 3H–P, 4D–F).

On the buccal side, the least worn teeth (GPIT/MA/17422 and SNSB-BSPG 2020 XCIV-1510) show a longer parastria and shorter mesostria (Fig. 3G). In contrast, similarly worn GPIT/MA/10989, 17367, and 17772 show an already closed


A
B1
B2
B3
C
D1
E1
F1
G
H
I
J
K1
L
M
N1
D2
D3
E2
F2
K2
K3
N2
N3
O1
P1
Q
R
S
T
O2
O3
P2
P3
10 mm
U
V1
V2
W1
X1
Y
Z1
AA1
AB
AC1
AD1
AE1
W2
W3
X2
X3
AF1
AG
AH
AI
Z2
AA2
AF2
AE2
AD2
AC2
AC3
AD3
AJ1
AK
AL
AM1
AN
AJ2
AJ3
AM2
AM3

parastria (parafossette) and an open and therefore longer mesostria (Figs. 3H, I, $4D_3$).

In occlusal view, the length of the hypoflexus is slightly shorter than the paraflexus, but both are curved mesially and almost meet lingually to the centre of the tooth (Figs. 3F–P, 4C, D_1, E_1, F_1).

The hypoflexus and paraflexus/fossette are highly variable. In five specimens they meet facing in a straight line (GPIT/MA/17772, 17422, 17163, SNSB-BSPG 2020 XCIV-3891 and 5375) (Figs. 3F–I, 4C). In contrast, five other specimens show a different pattern. In three of those teeth the curved ending of the paraflexus/fossette is oriented mesially to the hypoflexus (GPIT/MA/16935, 17081, and 10989), whereas in the two other teeth they are situated distally to the hypoflexus (GPIT/MA/10746 and SNSB-BSPG 2020 XCIV-1725). In general, the mesoflexus/fossette of the P4 is curved and elongated far to the posterior occlusal tooth margin. The metafossette is encompassed by the mesoflexus/fossette and relatively short. In the deeply worn GPIT/MA/10746 para- and mesofossette are more irregular and wavier in shape (Fig. 3P).

Only in one specimen with both P4s (GPIT/MA/17163) in situ, two additional fossettes are exposed. The smaller fossette is situated in between the hypoflexus and the mesofossette and the larger one is located in the distolingual corner and perpendicular to the lingual ends of the para-, meso-, and metafossette as well as the hypoflexus (Figs. $2A_1$, 3L, M).

M1/2: The occlusal outline of upper M1/2 is longer (mesio-distally) than wide (bucco-lingually) in early wear stages; with further wear this ratio changes to wider than long (compare Figs. 3Q–AD, 4G–M, N_1).

The hypostria ends well above the crown base and is the longest stria (Fig. $4K_3$, N_3). Buccal striae are only present in early wear stages and thus very short, terminating within the first third of the tooth crown (Fig. $4K_2$, N_2). The parastria and metastria are very short and nearly non-existent in one very slightly worn M1/2 (GPIT/MA/13820; Figs. 3R, 4H). The similarly slightly worn M1/2SNSB-BSPG 2020 XCIV-5366 exhibits no parastria (and thus a primary parafossette) but a well-expressed (4 mm long) metastria (Figs. 3Q, 4G). The mesostria is the longest buccal stria, only present in M1/2of earlier wear stages (GPIT/MA/13820, 16134, 16845, SNSB-BSPG 2020 XCIV-1391, 1724, 5366, 5367, 5368, 5370, 5371, 5372 and 5377; Figs. 3Q–AA, 4G–M). In four of these (GPIT/MA/16134, 16845, SNSB-BSPG 2020 XCIV-1724 and 5366) an additional, but very short metastria is also exposed (Figs. 3Q, V–X, 4G, K).

Form and orientation of flexus and fossettes on the occlusal surface are quite similar to P4 but the parafossette is much smaller or missing in heavily worn M1/2(GPIT/MA/10731, 17163) while the hypoflexus is elongated. In two cases of M1/2, meso- and metaflexus/fossette are interconnected at mid length (GPIT/MA/13820 and SNSB-BSPG 2020 XCIV-1391; Figs. 3R, U, 4H, I); in one separate case they are fused at the terminal end of the metaflexus (GPIT/MA/16134; Fig. 3V). In the least worn M1/2 (GPIT/MA/13820 and SNSB-BSPG 2020 XCIV 5366), the para- and metafossette are of irregular outline (Figs. 3Q, R, 4G, H). Three slightly worn M1/2 show an additional tiny enamel column/stylid at the base of the mesostria (GPIT/MA/13820, SNSB-BSPG 2020 XCIV-5377 and 5368; Figs. 3R, Z, 4H, M). All M1/2 have three roots: one dominant lingual root and two small buccal roots (Fig. $4K_2$, N_2).

M3: The M3 is the shortest tooth of the toothrow (Fig. $4Q_2$, P_2). The occlusal outline of the M3 is square but slightly elongated distally. The hypostria ends well above the crown base and is the longest stria like in the other upper molars. Only in two specimens, representing unworn, unrooted and thus not fully developed M3, the hypostria ends very slightly above the crown base (SNSB-BSPG XCIV-1320 and 3388; Fig. $4O_2$, P_2). Buccal striae are short and terminate within the first third of the height of the tooth crown. The mesostria is the longest buccal stria, usually followed by the parastria.

The metastria is very short and only present in four lesser worn M3 where it is located at the distobuccal corner in three specimens (GPIT/MA/10990, 12562 and SNSB-BSPG 2020 XCIV-0446; Figs. 3AH, AI, AL, 4R) and slightly shifted to the posterior side in SNSB-BSPG 2020 XCIV-0415 (Figs. 3AG, 4Q).

The two unworn M3 show a para- and a mesoflexus/-stria but no metastria (and thus a primary metafossette) (SNSB-BSPG 2020 XCIV-1320; Figs. 3AF, $4P_1$, P_2) or a very short

← Fig. 4. Upper (**A**–**T**) and lower (**U**–**AM**) cheek teeth of the beaver *Steneofiber depereti* Mayet, 1908, from the early Later Miocene locality Hammerschmiede (Bavaria, Germany), local stratigraphic levels HAM 5 and HAM 4. Deciduous premolars: (**A**, **B**, **U**–**V**); premolars (**C**–**F**, **W**–**AA**); molars (**G**–**N**, **O**–**T**, **AB**–**AI**, **AJ**–**AN**). Occlusal (A, B_1, C, D_1–F_1, G–J, K_1, L, M, N_1–P_1, Q–U, **V**1–**X1,** Y, Z_1, AA_1, AB, AC_1–AF_1, AI–AH, AJ_1, AK, AL, AM_1, AN), lingual (B_2, D_2–F_2, K_3, N_3–P_3, W_3, X_3, AC_2, AD_3, AE_2, AF_2, AJ_3, AM_2), and buccal (B_3, D_3, K_2, N_2, O_3, P_2, V_2–X_2, Z_2, AA_2, AC_3, AD_2, AJ_2, AM_3) views. Left DP4: (**A**) GPIT/MA/10744, HAM 5. Right DP4: (**B**) GPIT/MA/17763, HAM 4. Left P4: (**C**) SNSB-BSPG 2020 XCIV-3891, HAM 4; (**D**) GPIT/MA/10989, HAM 4; (**F**) GPIT/MA/10746, HAM 5. Right P4: (**E**) GPIT/MA/16935, HAM 4. Left M1/2: (**G**) SNSB-BSPG 2020 XCIV-5366, HAM 4; (**H**) GPIT/MA/13820, HAM 5. Right M1/2: (**I**) SNSB-BSPG 2020 XCIV-1391, HAM 4; (**J**) SNSB-BSPG 2020 XCIV-5372, HAM 4; (**K**) GPIT/MA/16845, HAM 4; (**L**) SNSB-BSPG 2020 XCIV-5370, HAM 4; (**M**) SNSB-BSPG 2020 XCIV-5368, HAM 4; (**N**) SNSB-BSPG 2020 XCIV-1726, HAM 4. Right M3: (**O**) SNSB-BSPG 2020 XCIV-3388, HAM 4. Left M3: (**P**) SNSB-BSPG 2020 XCIV-1320, HAM 4; (**Q**) SNSB-BSPG 2020 XCIV-0415, HAM 4; (**R**) GPIT/MA/12562, HAM 4; (**S**) GPIT/MA/16530, HAM 4; (**T**) SNSB-BSPG 2020 XCIV-1729, HAM 4. Right dp4: (**U**) GPIT/MA/13826, HAM 5; (**V**) GPIT/MA/10785, HAM 5. Right p4: (**W**) GPIT/MA/10745, HAM 4; (**X**) SNSB-BSPG 2020 XCIV-5362, HAM 4. Left p4 (**Y**) SNSB-BSPG 2020 XCIV-0487, HAM 4; (**Z**) SNSB-BSPG 2020 XCV-0303, HAM 5; (**AA**) GPIT/MA/09896, HAM 5. Right m1/2: (**AB**) GPIT/MA/16915, HAM 4; (**AD**) GPIT/MA/10987, HAM 4; (**AE**) GPIT/MA/16672, HAM 4; (**AF**) GPIT/MA/09906, HAM 5; (**AI**) GPIT/MA/12260, HAM 5. Left m1/2: (**AC**) SNSB-BSPG 2020 XCIV-5364, HAM 4; (**AG**) GPIT/MA/12342, HAM 5; (**AH**) GPIT/MA/13824, HAM 5. Right m3: (**AJ**) SNSB-BSPG 2020 XCIV-1722, HAM 4; (**AK**) GPIT/MA/13823, HAM 5; (**AN**) GPIT/MA/09907, HAM 5. Left m3: (**AL**) GPIT/MA/17388, HAM 4; (**AM**) SNSB-BSPG 2020 XCIV-1719, HAM 4.

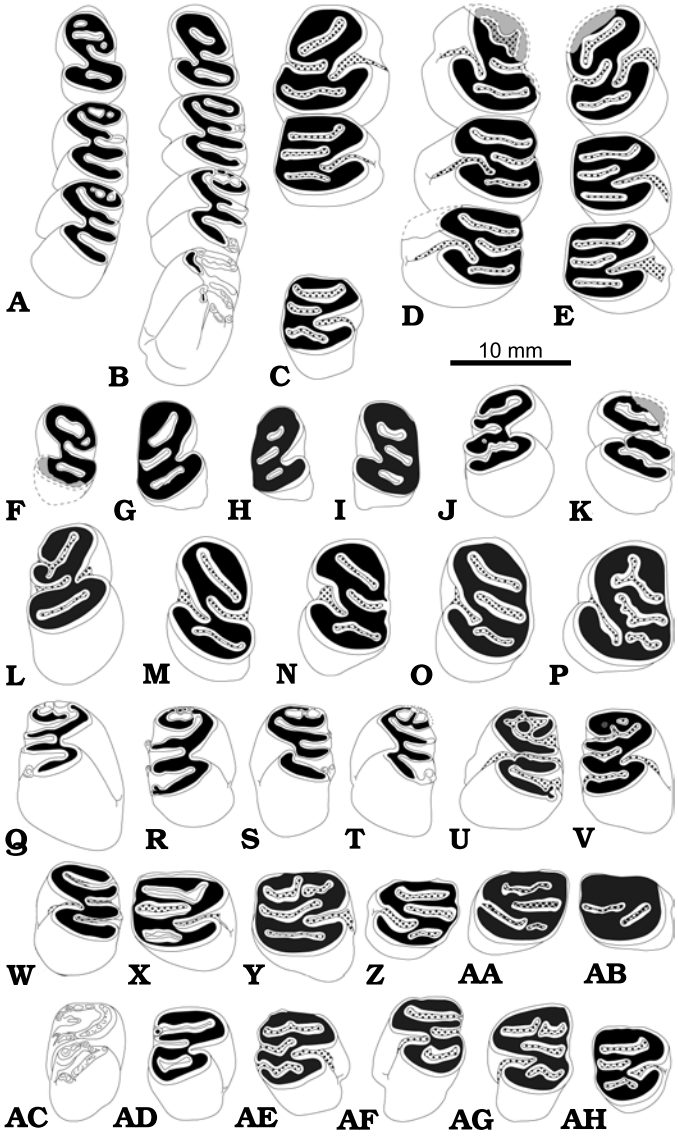

Fig. 5. Occlusal pattern of lower cheek teeth of the beaver *Steneofiber depereti* Mayet, 1908, from the early Late Miocene locality Hammerschmiede (Bavaria, Germany), local stratigraphic levels HAM 5 and HAM 4. Mandibular tooth rows (**A**–**E**), deciduous premolars (**F**–**I**), premolars (**J**–**P**), molars (**Q**–**AF**). Left dp4–m2: (**A**) GPIT/MA/17569, HAM 4; (**B**) GPIT/MA/16950, HAM 4. Right p4–m1 and m3, lacking m2: (**C**) GPIT/MA/09909, HAM 5. Left p4–m2: (**D**) GPIT/MA/17068, HAM 4. Right p4–m2: (**E**) GPIT/MA/16839, HAM 4. Left dp4: (**F**) GPIT/MA/10782, HAM 5; (**I**) SNSB-BSPG 2020 XCIV-5365, HAM 4. Right dp4: (**G**) GPIT/MA/13826, HAM 5; (**H**) GPIT/MA/10785, HAM 5. Right p4: (**J**) GPIT/MA/10745, HAM 5; (**L**) SNSB-BSPG 2020 XCIV-5362, HAM 4. Left p4: (**K**) GPIT/MA/10727, HAM 5; (**M**) GPIT/MA/13980, HAM 5; (**N**) GPIT/MA/09896, HAM 5; (**O**) SNSB-BSPG 2020 XCV-0303, HAM 5; (**P**) SNSB-BSPG 2020 XCIV-0487, HAM 4. Right m1/2: (**Q**) GPIT/MA/16915, HAM 4; (**R**) GPIT/MA/16672, HAM 4; (**V**) GPIT/MA/10987, HAM 4; (**X**) GPIT/MA/09903, HAM 5; (**Y**) SNSB-BSPG 2020 XCIV-5360, HAM 4; (**AB**) GPIT/MA/12260, HAM 5. Left m1/2: (**S**) GPIT/MA/09906, HAM 5; (**T**) GPIT/MA/10728, HAM 5; (**U**) SNSB-BSPG 2020 XCIV-5364, HAM 4; (**W**) GPIT/MA/09902, HAM 5; (**Z**) GPIT/MA/12342, HAM 5; (**AA**) GPIT/MA/13824, HAM 5. Right m3: (**AC**) SNSB-BSPG 2020 XCIV-1722, HAM 4; (**AD**) GPIT/MA/13823, HAM 5; (**AE**) GPIT/MA/10751, HAM 5; (**AH**) GPIT/MA/09907, HAM 5. Left m3: (**AF**) SNSB-BSPG 2020 XCIV-1719, HAM 4; (**AG**) GPIT/MA/17388, HAM 4. Enamel in white, dentine in black, cement as dotted area, completions in grey.

para-, a dominant meso- and a nearly as dominant metaflexus/-stria (SNSB-BSPG 2020 XCIV-3388; Figs. 3AE, $4O_1$, O_3). The former M3 shows a well-expressed paraflexus forming a "U", crossing the tooth buccolingually and then turning back mesially to the buccal margin. The latter M3 exhibits additional enamel columns/stylids within the mesostria, the metastria and at the lingual hypostria (Fig. 4O).

In more advanced wear stages, the paraflexus/fossette is randomly separated into a large mesial and a small distal fossette (GPIT/MA/10748, 10990, 12562 and SNSB-BSPG 2020 XCIV-0415; Figs. 3AG–AI, AK, 4Q, R). The slightly worn GPIT/MA/12562 shows an additional third paraflexus/-stria that is small but open buccally (Figs. 3AH, 4R). The most heavily worn M3 show in two cases only one hypo-, para-, meso-, and metafossette (GPIT/MA/16530 and SNSB-BSPG 2020 XCIV-1728; Figs. 3AM, AN, 4S) and in one case only hypo-, meso-, and a tiny metafossette (SNSB-BSPG 2020 XCIV-1729; Figs. 3AO, 4T).

All M3 have three roots, like the M1/2, with one dominant lingual root and two small buccal roots. Only the two unworn M3 (SNSB-BSPG 2020 XCIV-1320 and 3388) are still rootless and open at the base (Fig. $4O_3$, P_2).

Lower dentition: The material consists of 12 i2 (seven isolated tips, two fragments in situ, three complete teeth in situ), six dp4 (two still in their mandible), 18 p4 (four preserved in their mandible), 44 m1/2 and 14 m3, of which 18 molars are still in situ in ten jaw fragments (nine m1, seven m2 and two m3).

i2: Seven of the 12 lower incisor specimens include a preserved tip. In contrast to the upper incisor, the wear facet of the lower i2s is constantly angled and smooth. The wear facet is longer than in the upper I2 and extends from the labial enamel tip to the lingual edge. In cross section the lower incisors show a lingually elongated triangle. The lingual tip of the triangle is rounded and situated mesially. The mesial surface is nearly flat and parallel with the symphysis of the mandibles. The enamel face is convex in juvenile specimens (GPIT/MA/16436, 16985, and 17569), but it is "semiflattened" in older individuals, with a flattened mesial and a convex distal half of the enamel face.

dp4: All six dp4 are worn and para- and metafossetids are visible (Fig. 5A, B, F–H). Three of the dp4 are strongly worn and a closed mesoflexid is visible (GPIT/MA/13826, 10785, SNSB-BSPG 2020 XCIV-5365; Figs. 4U, V_1, 5G–I,). In the medium worn specimens, the mesoflexid is open and associated with a short mesostriid (Fig. 5A, B, F). All dp4 show a well-expressed hypoflexid with an associated hypostriid that terminates shortly above the crown base but extends as a groove until the tooth base (Fig. $4V_2$). The mesostriid is clearly longer than the meta- and parastriid (if present), but the hypostriid is always the longest. Synclines of the dp4 are never filled with cement. In all dp4 with preserved roots, two dominant main roots diverge mesially and distally, and a tiny third root protrudes buccally, mesially to the hypostriid (GPIT/MA/10785, 16950, and 17569; Fig. $4V_2$). GPIT/MA/17569 shows two additional small and circular

fossettids: one mesiobuccal (preparafossettid) and another distolingual (premesofossettid) (Fig. 5A).

p4: In premolars that are only slightly or medium worn, the typical eight-shaped occlusal outline is visible (Figs. $4W_1$, X_1, 5J–L). With increasing wear, the anterior part of the worn surface of the p4 extends in length mesially, whereas its width remains unchanged. With the last wear phase, an antero-lingual edge is forming that extends the mesiolingual part of the p4 up to the level of its distal part (Figs. 4Y, AA_1, 5C, D, N–P). The hypostriid always ends very close (approximately 3 mm) to the base of the crown. Slightly below the closure of the hypostriid, a well-expressed groove extends to the base of the tooth (Fig $4W_2$, X_2, Z_2, AA_2). The closure of the hypostriid can easily be overlooked in teeth of higher wear stages due to the increased accumulation of cementum in the striids; therefore, the continuing groove can be misinterpreted as an open hypostriid that reaches the tooth base.

Only in slightly worn p4 (GPIT/MA/10727, 10745), para- and metastriids of equal length are exposed and are closing within the first quarter of the tooth length (Figs. $4W_1$, W_3, 5J, K). In all specimens with more advanced wear stages the para- and metaflexid/striid are closed and their para- and metafossettid are visible. Generally, lower premolars show a well-developed mesostriid/flexid extending at least halfway down to the tooth base (Fig. $4W_3$, X_3). Only in the most heavily worn p4 (GPIT/MA/09896, SNSB-BSPG 2020 XCV-0303, 0487) the mesostriid/flexid is just closed and the mesofossettid is present (Figs. 4Y, Z_1, AA_1, 5N–P). In slightly worn p4 the hypoflexid is straight and diagonally oriented in medio-distal direction. The hypoflexid crosses approximately one third of tooth width and ends between the meso- and metaflexid. Only in the least worn premolars (GPIT/MA/10727, 10745 and SNSB-BSPG 2020 XCIV-5362), the hypoflexid ends in line with the ends of the meso- and metaflexid (Figs. $4W_1$, X_1, 5J–L). In GPIT/MA/10727 the meso- and metaflexid are fused with the hypoflexid (Fig. 5K). In moderate to heavy wear stages, the hypoflexid of lower premolars is hook-shaped and oriented more distally, never crossing the midline of tooth width. In these advanced wear stages, the mesoflexid/fossettid are more elongated, run mesially side by side with the terminating hypoflexid by forming a mesiobuccally oriented hook (GPIT/MA/09896, 13980, 16839 and SNSB-BSPG 2020 XCIV-0487; Figs. 4Y, AA_1, 5E, M, N, P), or stay straight (SNSB-BSPG 2020 XCV-0303; Figs. $4Z_1$, 5O). The mesoflexid is the shortest of the lingual flexids/fossettids and it slightly crosses the midline of the tooth width. The para- and metaflexids/fossettids run two thirds along the tooth width before they terminate. The shape of the paraflexid/fossettid on the occlusal surface is variable, showing a straight course or a convex (GPIT/MA/16839; Fig. 5E) to concave (GPIT/MA/09909; Fig. 5C) hook-shaped orientation. The metaflexids/fossettids are slightly undulating. In SNSB-BSPG 2020 XCIV-0487 all lingual fossetids are heavily undulating (Figs. 4Y, 5P).

m1/2/3: The typical outline of the lower molars is rectangular. The hypostriid/flexid is the longest striid/flexid and ends shortly above the crown base and closes to a hypofossetid without any lingual groove in contrast to the p4. The mesostriid is always longer than the para- and metastriid, both of which having the same length. Para- and metastriid are only present in the first millimetres of wear and they close within the first fourth of the tooth crown length. In contrast the mesostriid continues downwards until it closes before reaching half of the tooth crown height in m1/2 (Fig. $4AC_2$, AD_3, AE_2, AF_2,), but surpasses the half length of the crown height in m3 (Fig. $4AJ_3$, AM_2). The latter is bucco-lingually slightly narrower and approximately 20% shorter in crown height than a typical m1/2 (compare Fig. $4AC_2$, AC_3, AJ_2, AJ_3, AM_2, AM_3). In unworn and slightly worn molars, some special features in lingual flexids/fossettids are obvious: unworn molars show a U-shaped paraflexid that is oriented transversally on the occlusal surface, nearly reaching the buccal margin until it is reversing mesially all way back near the lingual tooth margin (Figs. 4AB, AC_1, AJ_1, 5B, Q, U, AC). In slightly worn m1/2 this "U" is divided and yields a typical straight transversal paraflexid and one elongated preparafossettid (Figs. $4AE_1$, 5B, R). With continuing wear this preparafossettid splits in two preparafossettids, a lingual and a buccal preparafossettid (GPIT/MA/09906, 10728, 10987, and 17569 [m1]; Figs. $4AF_1$, AD_1, 5A, S, T, V). In a single case a third preparafossettid appears (GPIT/MA/17569 [m2]; Figs. 5A, $6C_2$). Another singular specimen shows a Y-shaped paraflexid where the two endings encompass the buccal preparafossetid. Furthermore, the same m1/2 shows a second, lingual preparafossetid that is barely visible and nearly worn out (GPIT/MA/10987; Figs. 4AD, 5V). All preparafossettids are removed due to tooth wear before any lingual flexid closes. The medium worn GPIT/MA/17388 (m3) and the heavily worn SNSB-BSPG 2020 XCIV-5360 (m1/2) exhibit an interrupted parafossetid that is split into a lingual and a buccal parafossetid of equal dimensions (Figs. 4AL, 5Y, AG). In the most heavily worn molar only a hypo- and mesofossette is present (GPIT/MA/12260) (Figs. 4AI, 5AB). Three molars show tiny additional enamel columns or stylids at the lower ends of some lingual striids (GPIT/MA/16672, m1/2: parastriid and mesostriid; Figs. $4AE_1$, AE_2, 5R; GPIT/MA/09906, m1/2: parastriid and mesostriid, Figs. $4AF_1$, AF_2, 5S; GPIT/MA/13823, m3: only one stylid at the paraflexid, Figs. 4AK, 5AD). In general, paraflexid/fossettid, mesoflexid/fossettid and metaflexid/fossettid are straight or slightly undulating and transversely oriented on the occlusal surface.

Mandibles: The description of the mandible is mainly based on the four better preserved specimens: a nearly complete right mandible comprising of the angular process, part of the coronoid process, i2 and m1 (GPIT/MA/13813, Fig. 6A); a well-preserved right mandible with articular process, p4, m1, and m3 (GPIT/MA/09909, Fig. 6B); a mandible fragment with i2 (fragment) and p4–m2 (GPIT/MA/17068, Fig. 6D); and a juvenile left mandible with i2 and dp4–m2 (GPIT/MA/17569, Fig. 6C). In addition to that, the mandibular material consists of two isolated articular processes (GPIT/MA/16586, 17215) and eight smaller mandibular

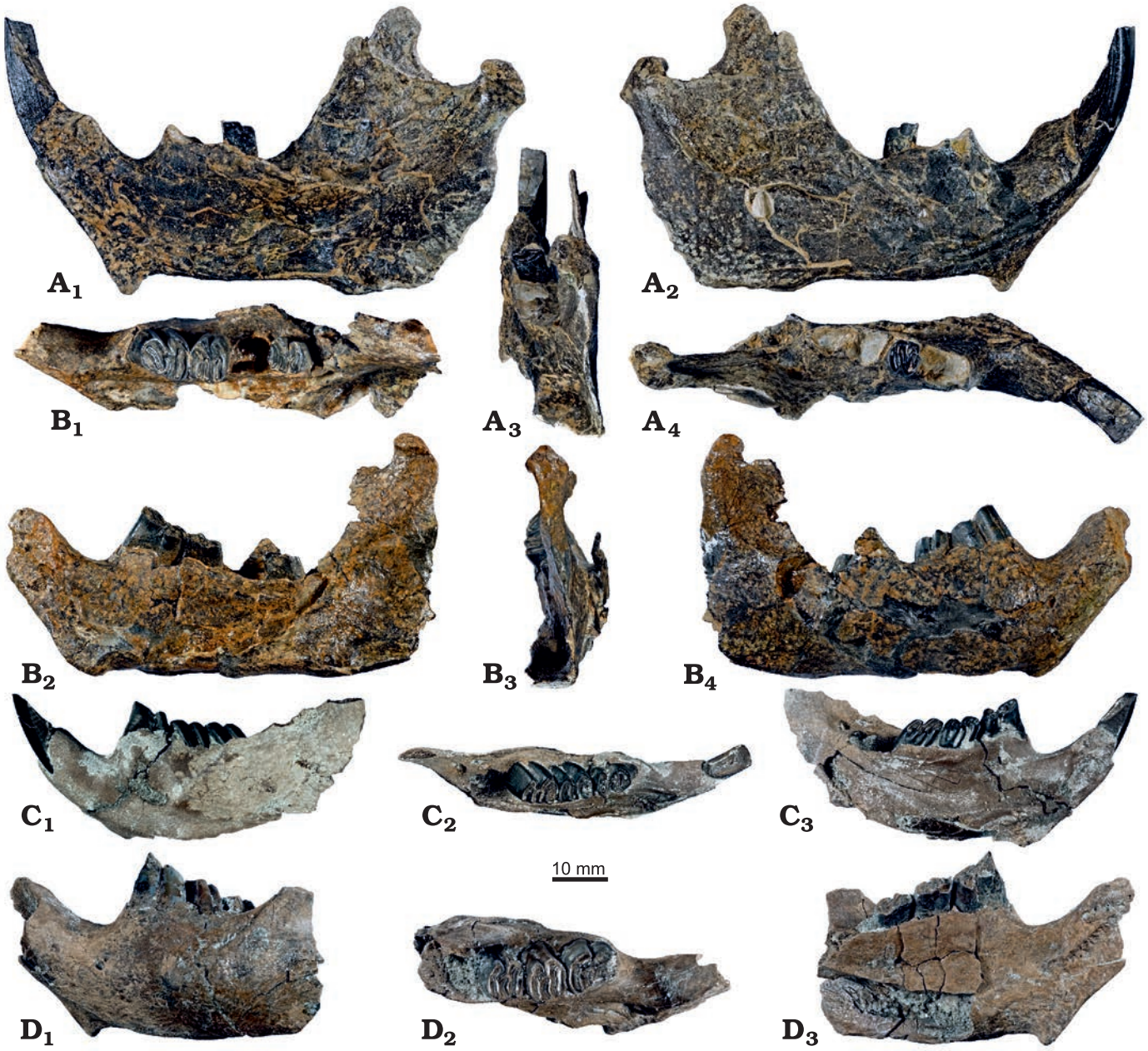

Fig. 6. Mandibles of the beaver *Steneofiber depereti* Mayet, 1908, from the early Late Miocene locality Hammerschmiede (Bavaria, Germany), local stratigraphic levels HAM 5 and HAM 4. **A**. GPIT/MA/13813, HAM 5, right mandible with angular process, part of the coronoid process, i2 and m1 in lingual (A_1), buccal (A_2), distal (A_3) and occlusal (A_4) views. **B**. GPIT/MA/09909, HAM 5, right mandible with angular process, p4, m1 and m3 in occlusal (B_1), lingual (B_2), distal (B_3) and buccal (B_4) views. **C**. GPIT/MA/17569, HAM 4, left mandible with i2, dp4, m1 and m2 (juvenile) in buccal (C_1), occlusal (C_2) and lingual (C_3) views. **D**. GPIT/MA/17068, HAM 4, left mandible with i2 (fragment), p4 (fragment), m1 and m2 in buccal (D_1), occlusal (D_2) and lingual (D_3) views.

fragments (GPIT/MA/10742, 16767, 16839, 16950, 17280, 18106, SNSB-BSPG 2020 XCIV-1494 and 2134).

In lateral view, the chin process is pointed postero-ventrally; it is situated anterior to the p4 in the older individuals (GPIT/MA/09909, 13813, and 17068; Fig. $6A_2$, B_4, D_1) and at the same height as the dp4 in the juvenile specimen (GPIT/MA/17569; Fig. $6C_1$). The mental foramen is situated anterior to the p4 (GPIT/MA/09909, 17068) and at the same height as the anterior margin of dp4 (GPIT/MA/17569). The m3 and parts of the m2 are hidden by the anterior margin of the coronoid process (GPIT/MA/09909, 17068, 17569) and a deep masseteric fossa is situated dorsal to the posterior end of the incisor (GPIT/MA/09909, 13813).

In lingual view, the angular shelf (crista pterygoidea) starts posterior to the m3; it bends horizontally and is expanded at the ventral margin (GPIT/MA/09909, 13813), thus a clear and distinct fossa for the pterygoid muscle is visible (Fig. $6A_1$, B_2). GPIT/MA/13813 has an elongated mandibular foramen that is situated posteriorly to the m3 at a crest starting at the lingual alveolar rim and continuing to the

condylar process (Fig. 6A$_1$, A$_4$). In the juvenile specimen (GPIT/MA/17569) this foramen is situated labially to this crest, directly posterior to the m3 alveolus (Fig. 6C$_2$, C$_3$). The symphysis is pointed to the chin process and expands dorsally. The occlusal margin of the toothrow is concave and slightly inclined posteriorly.

In posterior view, the coronoid and the angular processes are arranged in a vertical line (Fig. 6A$_3$). The articular process is shifted lingually to this line (GPIT/MA/09909, 13813; Fig. 6A$_3$, B$_3$).

Results and discussion

The taxonomic differentiation of fossil castorids is mainly limited to a few dental and cranial characters (Hugueney 1999). In the present case the lower premolar (p4) exhibits the only character that allows to assign the material of the larger castorid from Hammerschmiede to *Steneofiber depereti*, and not *Chalicomys jaegeri*. In a further analysis, a metric comparison with other Miocene beavers focusing on lower premolars (p4) and mandibular tooth row length is conducted. Furthermore, the dp4/p4 tooth is permanently in use during the entire lifetime of the beaver and thus offers the possibility to analyse the complete dental "attritional" record for *Steneofiber depereti* from Hammerschmiede from birth to death in a mortality analysis.

Comments on the genus *Steneofiber*.—The dental morphology of *Steneofiber depereti* is very similar to *Chalicomys jaegeri*; therefore, the distinction between the two genera remains difficult. Generally, *Chalicomys jaegeri* is considered to be the successor of *Steneofiber depereti* (Ginsburg 1971; Stefen 1997; Mörs and Stefen 2010). So far, the following features are usually used to distinguish *Steneofiber* spp. from *Chalicomys* spp.: increasing hypsodonty in *Chalicomys* spp.; development of a clear tetralophodont pattern with well-expressed striids on the lingual side in *Chalicomys* spp.; and cement filling of the striids even in early wear stages in *Chalicomys* spp. (Hugueney 1999; Casanovas-Vilar et al. 2008; Stefen 2009; Mörs and Stefen 2010). As already suggested by Mörs and Stefen (2010), the only clear difference is a hypostriid that always reaches the base of the tooth in *Chalicomys* spp. at least in its fourth lower premolar. Here we use this character as a potential synapomorphy of the clade including the genera *Chalicomys* and *Castor*. Therefore, all lower p4 with a hypostriid that does not reach the base of the tooth crown can be attributed to the genus *Steneofiber*.

Comments on the species of *Steneofiber*.—*Steneofiber* comprises two clearly distinguished species, the stratigraphically older mesodont *S. eseri* (MN 1–MN 2) and the younger hypsodont *S. depereti* (MN 3–MN 10). Both species are also characterized based on their dental metric data (Hugueney 1999). However, a third species, *S. subpyrenaicus* was discussed by Mörs and Stefen (2010) and they pointed out that

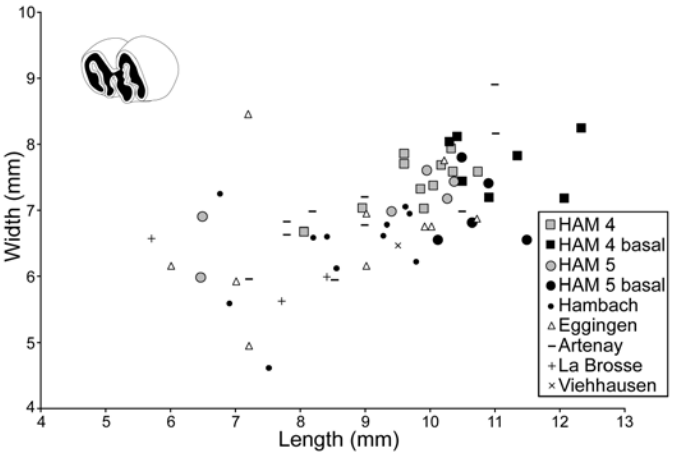

Fig. 7. Length/width dimensions of lower premolars of the beaver *Steneofiber depereti* Mayet, 1908, from the early Late Miocene locality Hammerschmiede (Bavaria, Germany), local stratigraphic levels HAM 5 and HAM 4, compared to other *S. depereti* material from Miocene localities in France and Germany. Data for Hambach from Mörs and Stefen (2010), for Eggingen-Mittelhart from Sach and Heizmann (2001) and Mörs and Stefen (2010), for Artenay from Mörs and Stefen (2010), for La Brosse from Ginsburg et al. (2000), and for Viehhausen from Seemann (1938). Measurements for HAM 5 and HAM 4 material is additionally compared by occlusal (grey) and basal (black) tooth measurements. Measurements for Hambach and Eggingen-Mittelhart contain both occlusal and basal tooth measurements. Data for Artenay, La Brosse and Viehhausen only include occlusal measurements.

the material of *S. subpyrenaicu*s might be undiagnostic or conspecific with *S. depereti*. We agree with Mörs and Stefen (2010) about their proposal that a subspecies differentiation should not be used for the European *Steneofiber* species, especially *S. depereti*. Since the morphology and metrics of the larger Hammerschmiede beaver correspond to the usual variability of *S. depereti* (Fig. 7), we assign the material described here to this species.

Tooth differences between *Chalicomys jaegeri* and *Steneofiber depereti* and the impact of increased cement filling.—*Chalicomys jaegeri* from the type locality Eppelsheim is characterized by hypsodont teeth with a hypostriid extending to the crown base, three well-expressed lingual striids and conspicuous cement in the synclines of the teeth already at early wear stages (Hugueney 1999; Stefen 2009; Mörs and Stefen 2010). According to previous studies, *Steneofiber depereti* exhibits subhypsodont to hypsodont teeth, closed hypostria/-iids, and only a labial mesostriid; it further lacks substantial cement in the synclines (Mayet 1908; Ginsburg 1971; Stefen 1997; Hugueney 1999; Sach and Heizmann 2001; Mörs and Stefen 2010). In the present sample from Hammerschmiede, the cheek teeth of a large castorid are subhypsodont to hypsodont. Lower cheek teeth of the Hammerschmiede beaver comprise three lingual striids with a dominant mesostriid and small additional para- and metastriids, but these are not as dominant and long as in *Chalicomys jaegeri* from Eppelsheim (Hugueney 1999; Stefen 2009) or Soblay (see Hugueney 1999: fig. 28.6E1). Furthermore, cheek teeth of the large beaver from

Table 2. Material list with dimensions (in mm) of upper and lower teeth of the beaver *Steneofiber depereti* Mayet, 1908, from the early Late Miocene locality Hammerschmiede (Bavaria, Germany) and the local stratigraphic levels HAM 5 and HAM 4. L, left; R, right. Cement codes the occurrence of cement filling in cheek teeth flexids with (0) no cement, (1) first, faint traces of cement, and (2) complete filling with cement; wear stages are defined as (1), unworn: no wear can be observed, deciduous dentition in use, (2) slightly worn: first occlusal contact, (3) worn: para/metaflexus/-id is closing or just closed, (4) medium worn: mesoflexus/-id is closing or just closed, (5) deeply worn: hypoflexus/-id is near to closing, (6) heavily worn: hypoflexus/-id is closed; length occlusal, mesio-distal length at occlusal surface of cheek teeth and length across anterior enamel band for incisors; length at base, mesio-distal length at basal tooth position (where possible); width occlusal, bucco-lingual width at occlusal surface of cheek teeth and incisors; width at base, bucco-lingual width at basal tooth position (where possible). Estimated values of measurements are marked by an asterisk (*).

Tooth position		Repository number	Layer	Cement [0–2]	Wear stage [1–6]	Occlusal		Base	
						length	width	length	width
I2	R	GPIT/MA/17456	HAM 4				6.87		
		GPIT/MA/17807	HAM 4			6.49	6.24		
		SNSB-BSPG 2020 XCIV-661	HAM 4			7.06	7.42		
		GPIT/MA/10753	HAM 5			5.77	5.85		
	L	GPIT/MA/10749	HAM 5			6.84	6.4		
DP4	R	GPIT/MA/17763	HAM 4	0	3	6.61	5.45	5.08	7.82
		SNSB-BSPG 2020 XCIV-0879	HAM 4	0	3	6.24	4.19	5.58	7.42
		SNSB-BSPG 2020 XCIV-1731	HAM 4	0	4		7.1		
	L	GPIT/MA/12416	HAM 4	0	3	6.59	4.48	6.8	9.82
		GPIT/MA/12489	HAM 4	0	4		5.88		8.45
		GPIT/MA/10744	HAM 5	0	3	6.1	5.51	5	7.61
		GPIT/MA/10781	HAM 5	0	4	5.76	6	5.6	7.52
P4	R	SNSB-BSPG 2020 XCIV-1510	HAM 4	1	2			7.99	8.21
		GPIT/MA/17367	HAM 4	1	3			8.26	9.45
		GPIT/MA/17422	HAM 4	2	4	9.19	8.11	7.95	9.28
		GPIT/MA/17772	HAM 4	2	4	8.92	8.81	8.02	9.84
		GPIT/MA/16935	HAM 4	2	4	8.96	9.58	8.01	9.15
		GPIT/MA/17081	HAM 4	2	4	8.5	8.33	7.59	8.83
		GPIT/MA/17163-2	HAM 4	2	4	7.74	8.94		
	L	GPIT/MA/10989	HAM 4	1	3	7.95	7.39	8.2	8.94
		GPIT/MA/17205	HAM 4	2	4	8.43	9.05	8.35	8.95
		GPIT/MA/17163-1	HAM 4	2	4	7.62	8.9		
		SNSB-BSPG 2020 XCIV-1725	HAM 4	1	5	9.56*	8.74*	7.62	8.38
		GPIT/MA/16979	HAM 4	2	5	8.42	9.32		
		SNSB-BSPG 2020 XCIV-3891	HAM 4	2	1	7.61	7.74	8.05	8.66
		SNSB-BSPG 2020 XCIV-5375	HAM 4	2	3	8.63	7.96	7.67	8.44
		GPIT/MA/10746	HAM 5	2	6	8.36	9	7.68	8.1
M1	R	GPIT/MA/17163-1	HAM 4	2	5	5.5	7.75		
	L	GPIT/MA/17367	HAM 4	1	4			5.47	7.7
M1–M2	R	GPIT/MA/16845	HAM 4	1	3	6.52	5.85	5.47	7.27
		SNSB-BSPG 2020 XCIV-1391	HAM 4	2	3	6.44	5.76	5.3	6.89
		GPIT/MA/17358	HAM 4	2	4	6.12	7.53	6.02	7.43
		SNSB-BSPG 2020 XCIV-1727	HAM 4	2	4	5.93	5.96	5.61	6.76
		SNSB-BSPG 2020 XCIV-1726	HAM 4	1	5	5.94	7.9	5.58	7.8
		SNSB-BSPG 2020 XCIV-5368	HAM 4	1	3	6.04	5.4	5.13	6.77
		SNSB-BSPG 2020 XCIV-5370	HAM 4	2	3	6.56	6.3	5.77	7.79
		SNSB-BSPG 2020 XCIV-5372	HAM 4	1	3	6.24	5.2	4.98	6.53
		SNSB-BSPG 2020 XCIV-5369	HAM 4	1	4	6.18	6.58	5.71	6.94
		SNSB-BSPG 2020 XCIV-5367	HAM 4	1	1	6.2	4.59	6.18	6.96
		SNSB-BSPG 2020 XCIV-5377	HAM 4	2	3	6.22	6.72	5.23	7.69
		SNSB-BSPG 2020 XCIV-5376	HAM 4	2	4	6.51	6.46	6.25	6.92
		SNSB-BSPG 2020 XCIV-5378	HAM 4	2	4	6.45	6.99	6.41	7.52
		SNSB-BSPG 2020 XCIV-5374	HAM 4	2	5	6.13	7.69	5.91	6.84
		SNSB-BSPG 2020 XCIV-4059	HAM 4	2	4	5.73	7.37	5.45	7.1
		GPIT/MA/12604	HAM 5	1	4	6.18	6.76	5.58	7.47
		GPIT/MA/13825	HAM 5	0	4	5.93	6.37	5.76	6.41

M1–M2	L	SNSB-BSPG 2020 XCIV-1724	HAM 4	1	3	6.18	6.18	6.02	6.47
		GPIT/MA/16134	HAM 4	1	3	6.19	5.82	5.94	6.93
		GPIT/MA/16755	HAM 4	1	4	7.4	5.77	5.75	7.97
		GPIT/MA/12490	HAM 4	2	4	5.54	6.47	5.22	6.6
		SNSB-BSPG 2020 XCIV-5366	HAM 4	1	1	6.1	4.3	5.7	6.63
		SNSB-BSPG 2020 XCIV-5371	HAM 4	1	2	5.93	5.02		
		GPIT/MA/13820	HAM 5	0	2	5.96	4.06	5.06	6.83
		GPIT/MA/10731	HAM 5	2	5	5.57	7.14	5.18	6.38
M2	R	GPIT/MA/17367	HAM 4	1	4			6.04	7.02
M3	R	SNSB-BSPG 2020 XCIV-1730	HAM 4	0	1	5.52	4.73	5.16	5.09
		GPIT/MA/10990	HAM 4	2	3	5.85	6.05	6.29	6.3
		SNSB-BSPG 2020 XCIV-0446	HAM 4	2	4	6.18	6.53	6.32	6.52
		SNSB-BSPG 2020 XCIV-3388	HAM 4	1	1	5.65	4.62	6.03	5.64
		SNSB-BSPG 2020 XCIV-5373	HAM 4	2	4	6.33	6.46	6.41	6.76
	L	SNSB-BSPG 2020 XCIV-1320	HAM 4	0	1	5.72	3.97	5.76	5.79
		SNSB-BSPG 2020 XCIV-0415	HAM 4	2	2	5.42	5.31	5.55	5.91
		GPIT/MA/12562	HAM 4	2	3	5.61	5.52	5.88	6.01
		GPIT/MA/16530	HAM 4	2	5	6.1	7	5.52	6.31
		SNSB-BSPG 2020 XCIV-1728	HAM 4	2	6			6.02	6.55
		SNSB-BSPG 2020 XCIV-1729	HAM 4	2	6			5.62	6.98
		GPIT/MA/10748	HAM 5	1	3	5.62	5.75	5.46	5.46
		GPIT/MA/12152	HAM 5	2	4	5.92	6.76	5.82	6.41
i2	R	GPIT/MA/16512	HAM 4			7.92	6.99		
		GPIT/MA/16928	HAM 4			7.3	6.95		
		GPIT/MA/16436	HAM 4			5.3	4.6		
		GPIT/MA/10742	HAM 5			7.19	7.47		
		GPIT/MA/10729	HAM 5			6.62	6.42		
		GPIT/MA/13813	HAM 5			7.88	7.16		
	L	SNSB-BSPG 2020 XCIV-1100	HAM 4			7.26	6.44		
		GPIT/MA/17569	HAM 4			5.38	4.54		
		GPIT/MA/16985	HAM 4			6.84	6.91		
		GPIT/MA/10743	HAM 5			4.14	4.15	4.94	4.47
dp4	R	GPIT/MA/10785	HAM 5	0	5	7.03	4.76		
		GPIT/MA/13826	HAM 5	0	4	8.26	5.51		
	L	GPIT/MA/16950	HAM 4	0	3	6.64	5.13	7.5	5.66
		GPIT/MA/17569	HAM 4	0	3	6.73	4.99	7.75	5.07
		SNSB-BSPG 2020 XCIV-5365	HAM 4	0	4	7.63	5.42		
		GPIT/MA/10782	HAM 5	0	3	6.56*	4.52*		
p4	R	GPIT/MA/18113	HAM 4	2	3	10.05	7.38		
		SNSB-BSPG 2020 XCIV-2276	HAM 4	2	3			10.9*	7.2*
		GPIT/MA/16839	HAM 4	2	3	9.85*	7.32		
		SNSB-BSPG 2020 XCIV-5362	HAM 4	2	3	8.95	7.02	11.35	7.82
		GPIT/MA/10745	HAM 5	0	2	6.47	5.98	10.9	7.4
		GPIT/MA/09909	HAM 5	2	3	9.95	7.6	10.5	7.79
	L	SNSB-BSPG 2020 XCIV-0179	HAM 4	2	3	9.9*	7.02*		
		SNSB-BSPG 2020 XCIV-1246	HAM 4	1	3	8.06*	6.67*	10.3*	8.04*
		GPIT/MA/17068	HAM 4	2	3	9.6*	7.7*		
		SNSB-BSPG 2020 XCIV-1494	HAM 4	2	3	9.6	7.86	10.42	8.11
		GPIT/MA/17352	HAM 4	2	4	10.35	7.58	12.07	7.18
		GPIT/MA/17296	HAM 4	2	4	10.74	7.58	10.5	7.44
		SNSB-BSPG 2020 XCIV-0487	HAM 4	1	5	10.33	7.94		
		SNSB-BSPG 2020 XCIV-3726	HAM 4	2	3	10.17	7.68	12.34	8.23
		GPIT/MA/10727	HAM 5	1	2	6.5*	6.9*		
		GPIT/MA/13980	HAM 5	2	3	10.27	7.17	11.5	6.55
		GPIT/MA/09896	HAM 5	2	4	9.42	6.97	10.13	6.55
		SNSB-BSPG 2020 XCV-303	HAM 5	2	4	10.38	7.43	10.65	6.81

m1	R	GPIT/MA/17280	HAM 4	1	4	6.67	7.17	6.8	8.04
		GPIT/MA/16839	HAM 4	2	4	6.7	7.1		
		GPIT/MA/09909	HAM 5	2	4	6.84	7.83	6.64	7.66
		GPIT/MA/13813	HAM 5	2	5	6.33	6.63		
	L	GPIT/MA/16950	HAM 4	0	2	6.18	5.57		
		GPIT/MA/17569	HAM 4	0	2	6.44	5.1		
		GPIT/MA/18106	HAM 4	2	4	6.38	6.52	6.14	6.88
		GPIT/MA/17068	HAM 4	2	4	6.9	7.12		
		SNSB-BSPG 2020 XCIV-1494	HAM 4	2	4	6.95	7.9		
m1–m2	R	GPIT/MA/16915	HAM 4	1	2	6.47	5.77	6.31	8.37
		GPIT/MA/16672	HAM 4	1	2	7.63	5.34	6.64	6.9
		GPIT/MA/10987	HAM 4	1	2	7.26	5.83	6.03	7.38
		SNSB-BSPG 2020 XCIV-1185	HAM 4	1	2	6.18	4.86	6.32	7.04
		SNSB-BSPG 2020 XCIV-1468	HAM 4	1	2	6.63	5.44	6.13	7.15
		SNSB-BSPG 2020 XCIV-1723	HAM 4	1	3	7.41	7.33	6.64	7.93
		SNSB-BSPG 2020 XCIV-3903	HAM 4	2	4	6.49	7.51	6.07	7.33
		SNSB-BSPG 2020 XCIV-5360	HAM 4	2	5	6.99	7.9	6.6	8.09
		SNSB-BSPG 2020 XCIV-5357	HAM 4	2	4	8.02	7.71	6.88	8.29
		SNSB-BSPG 2020 XCIV-5358	HAM 4	1	4	7.07	6.81	6.14	6.99
		GPIT/MA/09903	HAM 5	1	4	6.59	7.8	6.66	7.46
		GPIT/MA/13821	HAM 5	1	4	6.34	7.25	5.89	6.75
		GPIT/MA/12032	HAM 5	2	5	6.7	7.34		
		GPIT/MA/12260	HAM 5	2	6			5.94	7.25
	L	GPIT/MA/16908	HAM 4	1	3	7.32	6.26	6.03	7.34
		SNSB-BSPG 2020 XCIV-3572	HAM 4	1	2	6.36	5.6	5.8	6.82
		SNSB-BSPG 2020 XCIV-3745	HAM 4	2	3	6.59	7.04	7.67	5.93
		SNSB-BSPG 2020 XCIV-5364	HAM 4	1	1	7.1	5.49	6.61	7.84
		SNSB-BSPG 2020 XCIV-5363	HAM 4	2	4	6.73	7.79	6.46	7.86
		SNSB-BSPG 2020 XCIV-5359	HAM 4	2	3	7.18*	7.5*	7.17*	7.11*
		GPIT/MA/09906	HAM 5	1	2	6.3	5.26	5.94	6.86
		GPIT/MA/10728	HAM 5	0	2	6.38	4.55	6.03	7.13
		GPIT/MA/09902	HAM 5	1	3	6.02	5.91	5.99	6.88
		GPIT/MA/09897	HAM 5	1	3	6.46	6.95	6.97	6.64
		GPIT/MA/13822	HAM 5	1	4	6.22	6.94	6.09	7.17
		GPIT/MA/12342	HAM 5	1	5	5.74	7.08		
		GPIT/MA/10784	HAM 5	1	5	6.37	6.85	5.89	6.72
		GPIT/MA/13824	HAM 5	2	6			6.21	7.43
m2	R	SNSB-BSPG 2020 XCIV-2134	HAM 4	1	3	6.66	6.94		
		GPIT/MA/17280	HAM 4	1	4	7.42	6.8		
		GPIT/MA/16839	HAM 4	2	4	6.65	7.35		
	L	GPIT/MA/16950	HAM 4	0	2	6.38	5.22		
		GPIT/MA/17569	HAM 4	0	2	6.47	5.23		
		GPIT/MA/17068	HAM 4	2	4	6.8	7.25		
		SNSB-BSPG 2020 XCIV-1494	HAM 4	2	4	6.9	7.8		
m3	R	GPIT/MA/17666	HAM 4	1	4	6.86	6.01	6.27	6.4
		SNSB-BSPG 2020 XCIV-1722	HAM 4	1	1			6.2	6.54
		SNSB-BSPG 2020 XCIV-1720	HAM 4	1	4	6.91	6.46	6.51	6.01
		SNSB-BSPG 2020 XCIV-1721	HAM 4	2	4	6.6	6.63	6.56	6.49
		GPIT/MA/13823	HAM 5	0	3	6.22	6.39	6.5	6.55
		GPIT/MA/10751	HAM 5	2	3	6.68	6.7	6.57	6.24
		GPIT/MA/09909	HAM 5	2	4	6.64	6.5	7.23	5.92
		GPIT/MA/09907	HAM 5	2	5	6.75	6.38		
	L	GPIT/MA/16950	HAM 4	0	1	5.87	5.17	7.37	7.05
		SNSB-BSPG 2020 XCIV-0416	HAM 4	2	3	5.78	5.88	5.78	5.63
		SNSB-BSPG 2020 XCIV-1114	HAM 4	2	3	6.75	6.31	6.32	6.34
		GPIT/MA/17388	HAM 4	2	4	7.77	6.9	6.76	6.02
		SNSB-BSPG 2020 XCIV-1719	HAM 4	2	4	6.7	6.16	6.17	6.45
		SNSB-BSPG 2020 XCIV-5361	HAM 4	2	4	7.53	6.45	6.33	6.48

Hammerschmiede exhibit filling of cement in dental synclines that increases considerably with higher individual age. Table 2 and Figs. 2 and 3 show that deciduous (juvenile beavers) teeth never exhibit cement filling (Figs. 3A–E, 5A, B, F–I) and teeth assigned to WS 1 and WS 2 (juvenile and young adult beavers) comprise no or only slight cement agglomeration (Figs. 3Q, R, AE, AF, 5A, B, J, K, Q–T, AC–AD). At WS 3 and WS 4 (mature and senile beavers) this character state changes to first traces of cement (Figs. 3S–U, 5W, X) and completely cement-filled dental synclines (Figs. 3F–P, V–AD, AG–AO, 5C–E, L–P, U–V, Y–AB, AE–AH). This continuous increase of cement filling in dental synclines with higher wear stages and thus individual age indicates that the deposition of cement in Hammerschmiede beavers (and possibly any other European Miocene beaver) is a secondary effect during dental development. Compared to other European Miocene beaver species, the larger Hammerschmiede castorid represents an intermediate stage between the first forms of *Steneofiber* (*S. eseri*, *S. castorinus* and earlier forms of *S. depereti*; no cement in synclines), later forms of *Steneofiber depereti* (e.g., from Hambach, MN 5/6; with slight cement filling of dental synclines for individuals of higher ages) and *Chalicomys jaegeri* (cement-filled synclines already at juvenile individuals). A similar intermediate position becomes apparent when comparing the tooth crown height of cheek teeth (hypsodonty). The increase of cement accumulation possibly correlates with the increase of hypsodonty; therefore, it appears questionable to use this character as a diagnostic character at the species or even genus level in European castorids. Consequently, only one clear character remains to differentiate between *Chalicomys jaegeri* and *Steneofiber depereti*: the hypostriid, that closes before and does not reach the crown base in *Steneofiber depereti*, specifically in lower premolars.

Metric comparison of the lower premolar.—In addition to their identical morphology, the dimensions of the lower premolars from the two different Hammerschmiede layers are overlapping; the beavers from the HAM 5 and HAM 4 layers are thus considered as conspecific (Fig. 7). For further analyses, HAM 5 and HAM 4 material is merged. The age difference between these two layers is estimated to approximately 180 ka (Kirscher et al. 2016). The stratigraphically slightly younger beavers from HAM 4 exhibit the largest teeth in width and length (Fig. 7). This could indicate a slight tendency of body size enlargement through time or it might be explained with slightly changed environmental conditions as indicated by the wider and deeper river deposits of HAM 4 in contrast to the small rivulet of HAM 5 (Böhme et al. 2019; Mayr et al. 2020a).

The material from Hammerschmiede fits quite well into the size variability of other medium-sized Miocene beaver populations of Europe (Figs. 6, 7). The largest dimensions of the lower p4 from Hammerschmiede tend to be greater compared to other Miocene *Steneofiber* spp., but also *Chalicomys* spp. finds from Germany and France (Fig. 8).

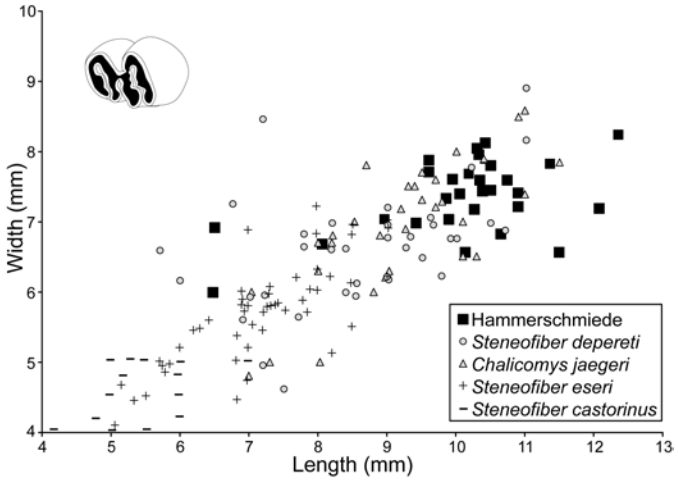

Fig. 8. Length/width dimensions of lower premolars of the beaver *Steneofiber depereti* Mayet, 1908, from the early Late Miocene locality Hammerschmiede (Bavaria, Germany), local stratigraphic levels HAM 5 and HAM 4, compared to *S. depereti* and several other castorid species from other European Miocene localities. Data for non Hammerschmiede *S. depereti* from Mörs and Stefen (2010) and citations therein, for *Chalicomys jaegeri* from Stefen (2009) and citations therein, for *Steneofiber eseri* from Stefen (1997), and for *Steneofiber castorinus* from Filhol (1879). Data points for all taxa resemble both occlusal and basal tooth measurements.

The smallest values for the lower p4 mesio-distal length from Hammerschmiede consist of occlusal measurements of slightly worn teeth. This observation is based on the typical morphology of the lower premolar, where in a buccal view the mesio-distal length increases heavily within the first wear stage. Therefore, occlusal measurements of unworn and very slightly worn p4 do not represent the typical tooth dimensions of the larger Hammerschmiede castorid.

Mandibular tooth row size.—In addition to the metrical analysis of lower premolars from different fossil Miocene localities, some authors compared the lengths of mandibular tooth rows at the occlusal surface and the alveolar length (Stefen 2009; Mörs and Stefen 2010; Stefen 2011). Following this approach, the available mandibular material of *Steneofiber depereti* from Hammerschmiede is added to the dataset and compared in the same way (Fig. 9). The length of the mandibular tooth rows of *S. depereti* from the combined HAM 4 and HAM 5 shows a similarly high intraspecific variability as other comparable comprehensive records of *Steneofiber* from Hambach (MN 5/6), Pontlevoy (MN 5), Ulm-Westtangente (MN 2a), and St. Geránd le Puy (MN 2a) (Fig. 9). In direct comparison, the small Early Miocene (MN 2) *Steneofiber eseri* and *Steneofiber castorinus* exhibit a clearly shorter mandibular tooth row. The lengths of *S. depereti* tooth rows from Hammerschmiede overlap with those of *S. depereti* (formerly *S. depereti caliodorensis*) from Chilleurs-aux-Bois (MN 3) and *S. depereti* from Hambach (MN 5/6). Considering the alveolar length, measurements of *S. depereti* (formerly *S. depereti janvieri*) from Denezé (base MN 3) do not overlap with those from Hammerschmiede. Furthermore, the tooth

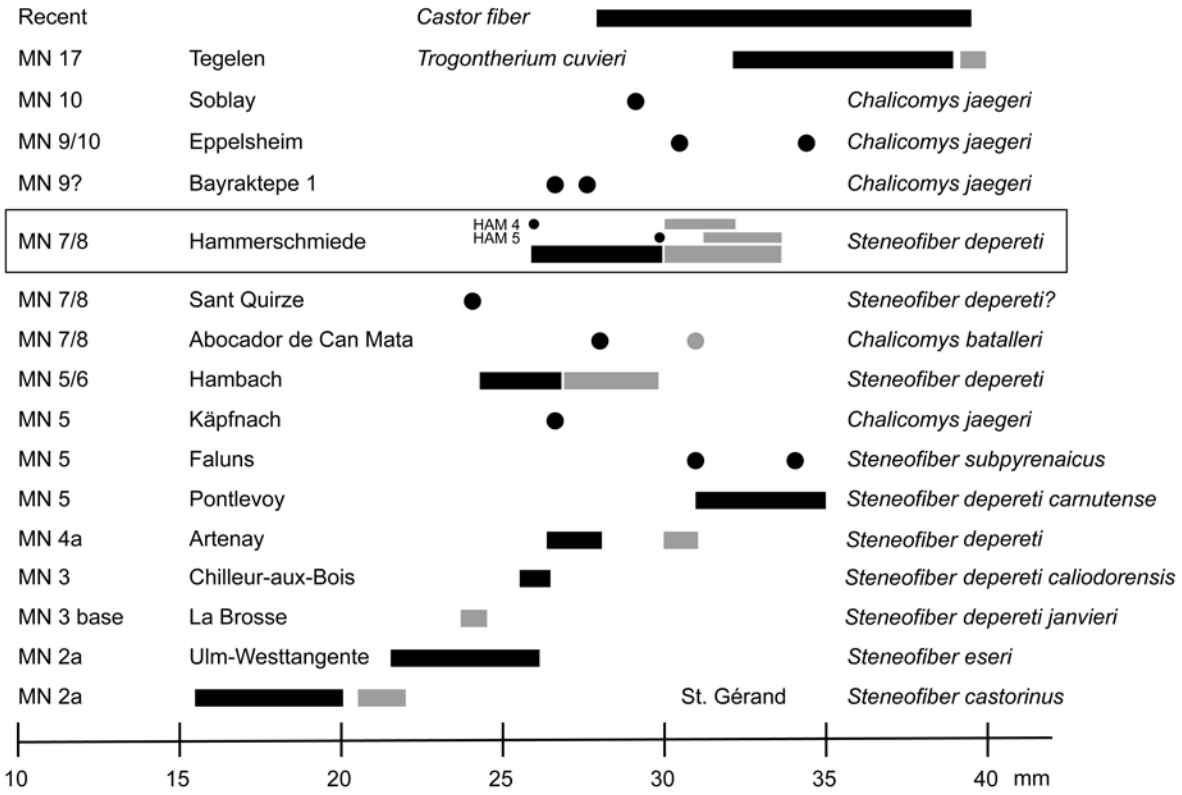

Fig. 9. Mandibular tooth row lengths of the beaver *Steneofiber depereti* Mayet, 1908, from the early Late Miocene locality Hammerschmiede (Bavaria, Germany), local stratigraphic levels HAM 5 and HAM 4, in comparison to representative European Miocene castorid species. Occlusal surface lengths are given as single measurements (black dots) or ranges (black bars). Alveolar lengths are given in grey dots or bars respectively. Measurements adapted from Stefen (2009), Mörs and Stefen (2010), Stefen (2011), and citations therein. Biostratigraphic positions of the localities according to the Mammal Neogene (MN) zones (sensu Mein 1975).

row lengths of the Early Miocene material from Käpfnach (MN 5) assigned to *Chalicomys jaegeri*, the Late Miocene *Chalicomys jaegeri* from Bayraktepe 1 (MN 9?), Soblay (MN 10) and Eppelsheim (MN 9/10), and also *Chalicomys batalleri* from Abocador de Can Mata (MN 7/8) are within the size range of Hammerschmiede mandibular tooth rows.

Wear stages of lower premolars and their step-length relation.—The highly different states of preservation of the dental material make it difficult to gather age groups based on tooth abrasion by measuring the tooth height directly. In order to include most available tooth specimens, the age groups are characterized by defined changes in the occlusal patterns of the cheek teeth depending on their dental wear stages. To avoid data duplication by multiple counting of individuals, the analysis is restricted to the lower dp4/p4 tooth position. Furthermore, this tooth position provides the only mortality record from birth (deciduous dentition) to death (permanent dentition). Morphological characters that define the wear stages of the p4 are not equally distributed along the entire tooth height. Therefore, the absolute age information differs according to the actual step-length between the wear stages (Fig. 10). In the least worn and isolated specimens of lower p4 (GPIT/MA/10727 and 10745) the absolute distribution of wear stages can be estimated by "percentage of dental lifespan" with the wear stages according to a maximum tooth height plus the lifetime of a juvenile individual with the dp4 still in use.

WS 1 represents the time range when a deciduous premolar (dp4) is used by a juvenile beaver (p4 is unerupted and unused at this stage). To avoid potential individual duplication by counting shed out deciduous teeth, which therefore do not represent the time of death of the beaver individual, dp4 with resorbed roots were excluded from counting. The attritional lifetime of the dp4 (WS 1) (interval between time of tooth eruption and time when dp4 is shed out) is of unknown relation to the wear stages of the p4 (WS 2–6). The entire p4 tooth height represents 100%. The relation of direct measurements of the wear stage step lengths of the example p4s leads to following approximate step length proportions (Fig. 10): WS 2 is a short (17%) step-length compared to the longest WS 3 (33%) and WS 4 (28%). WS 5 (11%) and WS 6 (11%) exhibit the shortest step-lengths of the p4 with approximately one third of WS 3 (Fig. 10). In consequence, this means that with the beginning of WS 4, 50% of the absolute dental lifespan of the lower p4 is worn and with the end of WS 4, 77% of the available enamel tooth height is abraded. Finally, a tentative assignment of wear stages and age groups results in: WS 1, juvenile; WS 2, young/prime adult; WS 3, mature/elder; WS 4 and higher wear stages, old/senile.

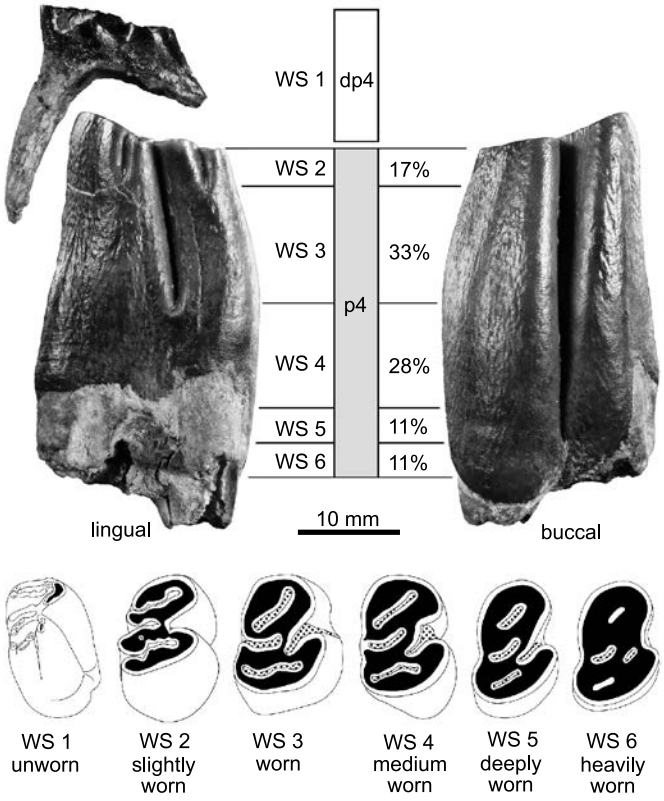

Fig. 10. Wear stages (WS) and step-length between between wear stages for the lower premolar dp4/p4 of the beaver *Steneofiber depereti* Mayet, 1908, from the early Late Miocene locality Hammerschmiede (Bavaria, Germany). The step-length of wear stages is given as an approximate percentage of the entire p4 tooth crown height (100%). Lower right dp4 (GPIT/MA/10785) in buccal (mirrored) view and lower left p4 (SNSB-BSPG 2020 XCIV-0487) for step-length of "age groups" definition in lingual and buccal views. WS 1, unworn: no wear can be observed, deciduous dentition in use; WS 2, slightly worn: first occlusal contact; WS 3, worn: para/metaflexus/id is closing or just closed; WS 4, medium worn: mesoflexus/id is closing or just closed; WS 5, deeply worn: hypoflexus/id is near to closing; WS 6, heavily worn: hypoflexus/id is closed. Occlusal pattern of lower right p4: WS 1, 3, 5 and 6: line drawings not based on specific specimens, WS 2: GPIT/MA/10745, WS 4: GPIT/MA/09896 (mirrored). WS 1–6 not to scale.

Mortality analysis.—In a following analysis, all unshed lower dp4 and p4 specimens from HAM 5 and HAM 4 strata representing the medium sized castorid *Steneofiber depereti* were counted and categorized by wear stage and an age-frequency distribution (Mortality profile) following Lyman (1994) was performed (Fig. 11).

In addition to the wear stage definitions as provided in the Material and Methods paragraph, the material representing WS 1 includes dp4s that are still in situ in the mandible, as well as isolated (used) dp4s, if they do not show signs of tooth resorption. Furthermore, unworn p4s would also relate to this age group and could duplicate dp4 data due to simultaneous occurrence, but no p4 in this wear stage is available from Hammerschmiede.

The mortality profiles according to the wear stages of the lower dp4/p4 specimens show different distributions in HAM 5 and HAM 4 (Fig. 11). In the HAM 4 profile, WS 1 (20%) and WS 3 (60%) dominate, while WS 4 (13.33%) and WS 5 (6.67%) are underrepresented and WS 2 and WS 6 are missing (Fig. 11). A different pattern occurs in the HAM 5 material, with high distributions in WS 1 (33%) and a consistent value for WS 2, WS 3 and WS 4 (22% each), with WS 4 being the highest available wear stage (Fig. 11).

The mortality profile of the HAM 4 layer complies with the typical U-shaped frequency distribution, referred to as "attritional" or "normal" mortality (Lyman 1994). This means that juvenile, mature and old individuals dominate the fossil material and young adults (WS 2) are lacking. This arrangement represents a natural ecological mortality (Lyman 1994). It can thus be assumed, that the HAM 4 river represents the natural ecosystem the beaver inhabited. A possible explanation for the low number of WS 1 and the complete absence of WS 2 material in HAM 4 could indicate a great ecological similarity of the larger Hammerschmiede castorid with the extant species of the *Castor*. Today's beavers mostly prefer deeper waters, which correspond roughly to rivers of 1st or 2nd stream orders (according to the classic stream order following Hack 1957) (Beier and Barret 1987; Dieter and McCabe 1989; Hartman 1996; Hartman and Törnlöv 2006), where HAM 4 is assumed to fit 2nd stream order. Since Hugueney and Escuillié (1995) already have documented K-strategy and two-year parental investment in the very early *Steneofiber eseri* from Montaigu-le-Blin (France, MN 2) and since a similar behaviour is known from the extant beaver (Hinze 1950), this behaviour can possibly also be assumed for *S. depereti* from Hammerschmiede. Compared to *Castor fiber*, WS 1 would then represent the first year of live where predation pres-

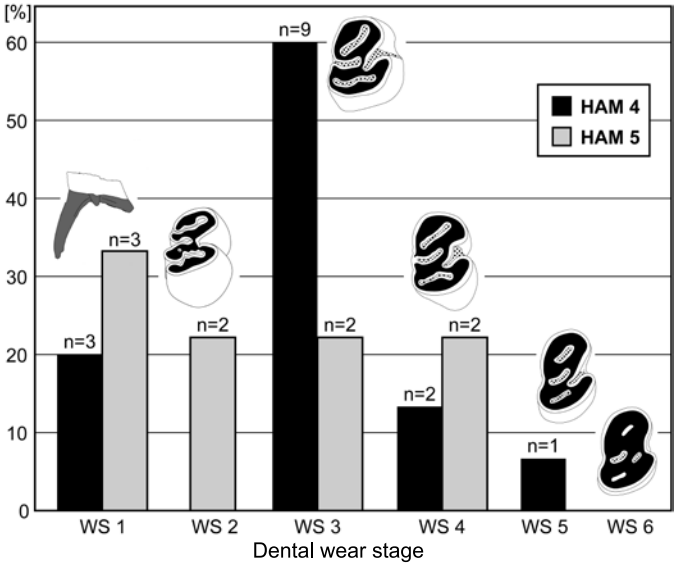

Fig. 11. Mortality profiles (age-frequency distribution) of the beaver *Steneofiber depereti* Mayet, 1908, from the early Late Miocene locality Hammerschmiede (Bavaria, Germany) based on lower dp4 and p4 tooth positions from the local stratigraphic levels HAM 5 and HAM 4. Each bar corresponds to an age class, defined by occlusal dental wear stages (WS 1–6). Vertical axis represents the percentage of individuals.

sure is moderate because of a small radius of movement close to the beaver lodge. WS 2 would include second year beavers, which migrate and are looking for their own territory, often on smaller tributaries (3rd stream order) because preferred territories are already occupied, as in extant beavers (Semyonoff 1951; Curry-Lindhal 1967; Żurowski and Kasperczyk 1986; Pupinnikas 1999; Gorshkov et al. 2002; Hartman and Törnlöv 2006). The greatest predation pressure in the *S. depereti* population of HAM 4 seems to be on prime age beavers (WS 3) with a continuous staircase slope towards old (WS 4) and senile (WS 5) individuals (Fig. 11), which indicates continuous colonisation by larger family groups in the habitat. In contrast to HAM 4, the HAM 5 age-frequency distribution cannot be assigned to a generalised mortality pattern (U-shaped or L-shaped according to Lyman 1994). In the mortality profile of HAM 5, teeth for WS 2 (n = 2) are present and of equal value with WS 3 and WS 4 (22% each). Except for the slightly higher value for WS 1, all available beaver ages in HAM 5 (WS 1–4) seem to show a similar predation pressure. A possible explanation for this observation could be that the HAM 5 rivulet was a sporadically colonised habitat of only small founder populations of *S. depereti*, where the locality would not match the preferred habitat requirements. This would be consistent with the observation that HAM 5 corresponds to a shallow river or rivulet of 3rd stream order, which would neither be the preferred habitat of extant beavers (Beier and Barret 1987; Dieter and McCabe 1989; Hartman 1996; Hartman and Törnlöv 2006), and thus would provide a niche for young adult beavers (especially WS 2) looking for a new territory.

Conclusions

The dental material of a medium sized castorid from the Hammerschmiede locality adds valuable morphological and metric data to the hitherto fragmentary record of European beavers of the early Late Miocene age. Furthermore, the material is characterised by a morphological intermediate stage between *Chalicomys jaegeri* and *Steneofiber depereti*. The still debated transitional evolution of *Steneofiber depereti–Chalicomys jaegeri–Castor fiber* implies that a differentiation between those taxa can be difficult (Mörs and Stefen 2010). The nominal types of this lineage, the early forms of *S. depereti* from the Early Miocene (MN 4) and the late forms of *C. jaegeri* from the Late Miocene (MN 9/10) are easily distinguishable. In contrast, the late forms of *S. depereti* and *C. jaegeri* share many dental characters (subhypsodont to hypsodont cheek teeth, three lingual striids, closure of roots at moderate or higher age, and synclines filled with cement at least at higher age) and can hardly be separated. In contrast, the Early Miocene European *Steneofiber eseri* and *Steneofiber castorinus*, characterized by a smaller size and mesodont cheek dentition, no cement in synclines, the absence of the three lingual striids, and the closure of roots at juvenile age, can be easily distinguished from both *S. depereti* and *C. jaegeri*. With the medium size Hammerschmiede castorid sample, the taxonomic distinction between the two latter species is reduced to one character of the lower premolar: a hypostriid that does not reach the crown base in *S. depereti*. Whether it is appropriate to differentiate two species at the genus level with only one character is questionable and beyond the scope of this study.

By categorising the dental wear stages of lower premolars of *S. depereti* from Hammerschmiede in an age-frequency distribution (Mortality analysis), it can be proposed, that the Hammerschmiede beaver shows similarities in demography and ecology, including similar habitat requirements, with extant beavers. The 2nd order stream HAM 4 can be interpreted as a typical beaver habitat with continuous occupation by larger family groups (temporal and spatial), while the 3rd order stream HAM 5 is interpreted as not optimally matching the habitat requirements of *S. depereti*., resulting in a discontinuous occupation by smaller family groups, and thus primarily offering a niche for young adult beavers looking for a new territory.

Finally, the beavers from the locality Hammerschmiede in Southern Germany are part of a highly diverse river, rivulet and floodplain ecosystem of the early late Miocene that is an ideal environment for castorids. Thus, it is not surprising, that a second, but smaller beaver species, *Euroxenomys minutus*, is also inhabiting this environment. Due to similarities in the ecological behaviour of castorids, most fossil beaver sites contain only one species, and only a few localities comprise two or more species (Rekovets et al. 2020). If more than one beaver taxon is found at a fossil site, usually one is much more abundant. This is not the case for the Hammerschmiede beavers. Here, both the large *S. depereti* and the small *E. minutus* are frequently found.

Acknowledgements

The authors wish to thank Ingmar Werneburg (GPIT) for providing access to the specimens under his care (GPIT and SNSB-BSPG stored at GPIT). Further, we wish to thank Wolfgang Lechner (Nawilab, Trostberg, Germany) for providing recent reference material. We thank Henrik Stöhr (GPIT) for the preparation of the specimens and Agnes Fatz (Senckenberg Center HEP, Tübingen, Germany) for assistance and access to the photo laboratory. We further acknowledge all participants of the numerous excavations in the Hammerschmiede fossil site, who helped to detect and collect the studied material. The excavations and associated research were supported by the Bavarian State Ministry of Research and the Arts and by the Bavarian Natural History Collections (SNSB). We would also like to thank Ilona Gold, Christian Dietzel, Panagiotis Kampouridis, Felix Augustin, and Andreas Matzke (all GPIT) for fruitful discussions and improvement of the manuscript. Finally, we thank the editor Olivier Lambert (Royal Belgian Institute of Natural Sciences, Belgium), Clara Stefen (Senckenberg Naturhistorische Sammlungen Dresden, Germany), and an anonymous reviewer for helpful comments and suggestions on the manuscript.

References

Aldana Carrasco, E. 1992. Los Castoridae (Rodentia,Mammalia) del Neógeno de Cataluña (España). *Treballs del Museu de Geologia de Barcelona* 2: 99–141.

Beier, P. and Barrett, R.H. 1987. Beaver habitat use and impact in Truckee River Basin, California. *Journal of Wildlife Management* 51: 794–799.

Böhme, M., Spassov, N., DeSilva, J.M., and Begun, D.R. 2020. Reply to: Reevaluating bipedalism in *Danuvius*. *Nature* 586: E4–E5.

Böhme, M., Spassov, N., Fuss, J., Tröscher, A., Deane, A.S., Prieto, J., Kirscher, U., Lechner, T., and Begun, D.R. 2019. A new Miocene ape and locomotion in the ancestor of great apes and humans. *Nature* 575: 489–493.

Bowdich, T.E. 1821. *An Analysis of the Natural Classifications of Mammalia for the Use of Students and Travellers*. 115 pp. J. Smith, Paris.

Casanovas-Vilar, I. and Alba, D.M. 2011. The never-ending problem of Miocene beaver taxonomy. *Acta Palaeontologica Polonica* 56: 217–220.

Casanovas-Vilar, I., Alba, D.M., Almécija, S., Robles, J.M., Galindo, J., and Moyà-Solà, S. 2008. Taxonomy and paleobiology of the genus *Chalicomys* Kaup, 1832 (Rodentia, Castoridae), with the description of a new species from Abocador De Can Mata (Vallès-Penedès Basin, Catalonia, Spain). *Journal of Vertebrate Paleontology* 28: 851–862.

Curry-Lindahl, K. 1967. The beaver, *Castor fiber* Linnaeus, 1758 in Sweden—extermination and reappearance. *Acta Theriologica* 12 (1): 1–15.

Dieter, C.D. and McCabe, T.R. 1989. Factors influencing beaver-lodge site selection on a prairie river. *The American Midland Naturalist* 122 (2): 408–411.

Fahlbusch, V. and Mayr, H. 1975. Microtoide Cricetiden (Mammalia, Rodentia) aus der Oberen Süßwasser-Molasse Bayerns. *Palaeontologische Zeitschrift* 49: 78–93.

Filhol, M.H. 1879. Etude des mammifères fossiles de Saint-Gérand-le-Puy (Allier). *Annales des Sciences géologiques* 10: 1–252.

Fischer von Waldheim, G. 1809. Sur l'Elasmotherium et le Trogontherium, deux animaux fossils et inconnus de la Russie. *Études palaeontologiques sur les environs de Moscou* 2: 250–268.

Franzen, J.L. and Storch, G. 1975. Die unterpliozäne (turolische) Wirbeltierfauna von Dorn-Dürkheim, Rheinhessen (SW-Deutschland); 1. Entdeckung, Geologie, Mammalia: Carnivora, Proboscidea, Rodentia. Grabungsergebnisse 1972–1973. *Senckenbergiana lethaea* 56: 233–303.

Freye, H.-A. 1959. Deskriptive Anatomie des Craniums vom Elbe-Biber (*Castor fiber albicus* MATSCHIE 1907). *Wissenschaftliche Zeitschrift der Martin-Luther-Universität Halle-Wittenberg. Mathematisch-naturwissenschaftliche* 8: 913–962.

Fuss, J., Prieto, J., and Böhme, M. 2015. Revision of the boselaphin bovid *Miotragocerus monacensis* Stromer, 1928 (Mammalia, Bovidae) at the Middle to Late Miocene transition in Central Europe. *Neues Jahrbuch für Geologie und Paläontologie Abhandlungen* 276: 229–265.

Geoffroy-Saint-Hilaire, E.-F. 1833. Considérations sur des ossements fossils la plupart inconnus, trouvés et observés dans les bassins de l'Auvergne. *Revue encyclopédique (Paris)* 59: 76–95.

Ginsburg, L. 1971. Sur l'évolution des *Steneofiber* (Mammalia, Rodentia) en France. *Comptes rendus de l'Académie des sciences, Paris, Série D: Sciences naturelles* 272: 2159–2161.

Ginsburg, L., Cheneval, J., Janvier, P., Pouit, D., and Sen, S. 2000. Les Vertébrés des sables continentaux d'âge orléanien inférieur (MN 3) de Mauvières à Marcilly-sur-Maulne (Indre-et-Loire), La Brosse à Meigné-le-Vicomte (Maine-et-Loire) et Chitenay (Loir-et-Cher). *Geodiversitas* 22: 597–631.

Gorshkov, Y.U., Gorshkov, D.Y., Easter-Pilcher, A.L., and Pilcher, B.K. 2002. First results of beaver (*Castor fiber*) reintroduction in Volga-Kama national nature Zapovednik (Russia). *Folia Zoologica* 51: 64–74.

Hack, J.T. 1957. Studies of longitudinal stream profiles in Virginia and Maryland. Shorter contributions to general geology. *U.S. Geological Survey Professional Paper* 294-B: 45–97.

Hartman, G. 1996. Habitat selection by European beaver (*Castor fiber*) colonizing a boreal landscape. *Journal of Zoology (London)* 240: 317–325.

Hartman, G. and Törnlöv, S. 2006. Influence of watercourse depth and width on dam-building behaviour by Eurasian beaver (*Castor fiber*). *Journal of Zoology (London)* 268: 127–131.

Hartung, J. and Böhme, M. 2022. Unexpected cranial sexual dimorphism in the tragulid *Dorcatherium naui* based on cranial material from the middle to late Miocene localities of Eppelsheim and Hammerschmiede (Germany). *PLOS ONE*. [published online, https://doi.org/10.1371/journal.pone.0267951]

Hartung, J., Lechner, T., and Böhme, M. 2020. New cranial material of *Miotragocerus monacensis* (Mammalia: Bovidae) from the late Miocene hominid locality Hammerschmiede (Germany). *Neues Jahrbuch für Geologie und Paläontologie Abhandlungen* 298: 269–284.

Heinrich, W.-D. and Maul, L.C. 2020. Mortality profiles of *Castor* and *Trogontherium* (Mammalia: Rodentia, Castoridae), with notes on the site formation of the Mid-Pleistocene hominin locality Bilzingsleben II (Thuringia, Central Germany). *Fossil Imprint* 76: 40–58.

Hemprich, W. 1820. *Grundriss der Naturgeschichte für höhere Lehranstalten*. 29 pp. August Rücker, Berlin.

Hinze, G. 1950. *Der Biber.* 216 pp. Körperbau und Lebensweise-Verbreitung und Geschichte Akademie-Verlag, Berlin.

Hugueney, M. 1999. Family Castoridae. *In*: G.E. Rössner and K. Heissig (eds.), *The Miocene Land Mammals of Europe*, 281–300.Verlag Friedrich Pfeil, Munich.

Hugueney, M. and Duranthon, F. 2012. Les Castoridae (Rodentia) de Sansan. *In*: S. Peigné (ed.), *Mammifères de Sansan. Mémoires du Muséum National d'Histoire Naturelle*, 95–118. Publications Scientifiques du Muséum, Paris.

Hugueney, M. and Escuillié, F. 1995. K-strategy and adaptive specialization in *Steneofiber* from Montaigu-le-Blin (dept. Allier, France; Lower Miocene, MN 2a, ±23 Ma): first evidence of fossil life-history strategies in castorid rodents. *Palaeogeography, Palaeoclimatology, Palaeoecology* 113: 217–225.

Jäger, G.F. 1835. *Ueber die fossilen Säugethiere, welche in Württemberg aufgefunden worden sind*. 70 pp. C. Erhard, Stuttgart.

Kargopoulos, N., Kampouridis, P., Lechner, T., and Böhme, M. 2021a. A review of *Semigenetta* (Viverridae, Carnivora) from the Miocene of Eurasia based on material from the hominid locality of Hammerschmiede (Germany). *Geobios* 69: 25–36.

Kargopoulos, N., Kampouridis, P., Lechner, T., and Böhme, M. 2021b. Hyaenidae (Carnivora) from the Late Miocene hominid locality of Hammerschmiede (Bavaria, Germany). *Historical Biology* [published online, https://doi.org/10.1080/08912963.2021.2010193]

Kargopoulos, N., Valenciano, A., Abella, J., Kampouridis, P., Lechner, T., Böhme, M. 2022. The exceptionally high diversity of small carnivorans from the Late Miocene hominid locality of Hammerschmiede (Bavaria, Germany). *PLOS ONE* 17 (7): e0268968.

Kargopoulos, N., Valenciano, A., Kampouridis, P., Lechner, T., and Böhme, M. 2021c. New early late Miocene species of *Vishnuonyx* (Carnivora, Lutrinae) from the hominid locality of Hammerschmiede, Bavaria, Germany. *Journal of Vertebrate Paleontology* 41. [published online, https://doi.org/10.1080/02724634.2021.1948858]

Kaup, J.J. 1832. Beschreibung dreyer Gattungen urweltlicher Nager des zoologischen Museums zu Darmstadt, welche von den jetzt lebenden Genera verschieden sind. *Isis* 9: 992–996.

Kaup J.J. 1833. Mitteilungen an Professor Bronn [letter to Bronn]. *Neues Jahrbuch für Mineralogie, Geognosie, Geologie und Petrefaktenkunde* 1833: 419–420.

Kirscher, U., Prieto, J., Bachtadse, V., Abdul Aziz, H., Doppler, G., Hagmaier, M., and Böhme, M. 2016. A biochronologic tie-point for the base of the Tortonian stage in Europe terrestrial settings: Magnetostratigraphy of the topmost Upper Freshwater Molasse sediments of the North Alpine Foreland Basin in Bavaria (Germany). *Newsletters on Stratigraphy* 49: 445–467.

Lambrecht, K. 1916. Die Gattung *Plotus* im ungarischen Neogen. *Mitteilungen aus dem Jahrbuche der königlichen ungarischen Geologischen Reichsanstalt* 24: 1–24

Lechner, T.S. and Böhme, M. 2020. *Castor*-like postcranial adaptation in an

uppermost Miocene beaver from the Staniantsi Basin (NW Bulgaria). *Fossil Imprint* 76: 128–164.

Linnaeus, C. 1758. *Systema naturae Per Regna Tria Naturae, Secundum Classes, Ordines, Genera, Species cum Characteribus, Differentiis, Synonymis, Locis.* 824 pp. Laurentius Salvius, Holmiae (Stockholm).

Lyman, R.L. 1994. *Vertebrate Taphonomy. Cambridge Manuals in Archaeology.* 524 pp. Cambridge University Press, Cambridge.

Mayet, L. 1908. Étude des mammifères miocènes des sables de l'Orléanais et des faluns de la Touraine. *Annales de l'Universitè de Lyon. Nouvelle Série, I. Sciences, Médecine* 24: 1–336.

Mayr, G., Lechner, T., and Böhme, M. 2020a. A skull of a very large crane from the late Miocene of Southern Germany, with notes on the phylogenetic interrelationships of extant Gruinae. *Journal of Ornithology* 161: 923–933.

Mayr, G., Lechner, T., and Böhme, M. 2020b. The large-sized darter *Anhinga pannonica* (Aves, Anhingidae) from the late Miocene hominid Hammerschmiede locality in Southern Germany. *PLOS ONE* 15 (5): 0232179.

Mayr, G., Lechner, T., and Böhme, M. 2022. Nearly complete leg of an unusual, shelduck-sized anseriform bird from the earliest late Miocene hominid locality Hammerschmiede (Germany). *Historical Biology.* [published online, https://doi.org/10.1080/08912963.2022.2045285].

Mayr, H. and Fahlbusch, V. 1975. Eine unterpliozäne Kleinsäugerfauna aus der Oberen Süßwasser-Molasse Bayerns. *Mitteilungen der Bayerischen Staatssammlung für Paläontologie und Historische Geologie* 15: 91–111.

Mein, P. 1975. Résultats du groupe de travail des vertébrés: Biozonation du Néogène méditerranéen à partir des mammifères. *In*: J. Senes (ed.), *Report on Activity of the RCMNS Working Groups (1971–1975)*, 78–81. Bratislava.

Mörs, T. and Stefen, C. 2010. The castorid *Steneofiber* from NW Germany and its implications for the taxonomy of Miocene beavers. *Acta Palaeontologica Polonica* 55: 189–198.

Pomel, A. 1847. Note sur des animaux fossiles découverts dans le département de l'Allier. *Bulletin de la Société géologique de France* 4: 378–385.

Prieto, J. 2012. The genus *Eomyops* Engesser, 1979 (Rodentia, Eomyidae) from the youngest deposits of the German part of the North Alpine Foreland Basin. *Swiss Journal of Palaeontology* 131: 95–106.

Prieto, J. and van Dam, J.A. 2012. Primitive Anourosoricini and Allosoricinae from the Miocene of Germany. *Geobios* 45: 581–589.

Prieto, J. and Rummel, M. 2009. Evolution of the genus *Collimys* Daxner-Hock, 1972 (Rodentia, Cricetidae) a key to Middle to Late Miocene biostratigraphy in Central Europe. *Neues Jahrbuch für Geologie und Paläontologie Abhandlungen* 252: 237–247.

Prieto, J., van den Hoek Ostende, L.W., Böhme, M., and Braze, M. 2011. Reappearance of *Galerix* (Erinaceomorpha, Mammalia) at the Middle to Late Miocene transition in South Germany: biostratigraphic and palaeoecologic implications. *Contributions to Zoology* 80: 179–189.

Pupinnikas, S. 1999. The state of the beaver (*Castor fiber*) populations and characteristics of beaver sites in Lithuania. *Acta Zoologica Lithuanica* 9: 20–26.

Rekovets, L., Kopij, G., and Nowakowski, D. 2009. Taxonomic diversity and spatio-temporal distribution of late Cenozoic beavers (Castoridae, Rodentia) of Ukraine. *Acta Zoologica Cracoviensia. Series A: Vertebrata* 52: 95–105.

Rekovets, L., Stefen, C., and Demeshkant, V. 2020. Beavers (Castoridae, Rodentia) from the late Miocene (MN 9) locality Grytsiv in Ukraine. *Fossil Imprint* 76: 165–173.

Roger, O. 1898. Wirbeltierreste aus dem Dinotheriensande der bayerisch-schwäbischen Hochebene. *Bericht des Naturwissenschaftlichen Vereins für Schwaben und Neuburg* 33: 1–46.

Sach, V.J. and Heizmann, E.P.J. 2001. Stratigraphie und Säugetierfauna der Brackwassermolasse in der Umgebung von Ulm (Südwestdeutschland). *Stuttgarter Beiträge zur Naturkunde Serie B (Geologie und Paläontologie)* 310: 1–95.

Samson, P. and Radulesco, C. 1973. Rémarques sur l'évolution des Castoridés (Rodentia, Mammalia). *In*: Traian Orghidan (ed.), *Livre du cinquantenaire de L'Insitut de Spéléologie "Emile Racovitza"*, 437–449. Academiae Republicii Socialiste România, Bucarest.

Schlosser, M. 1884. Die Nager des europäischen Tertiärs nebst Betrachtungen übder die Organisation und die geschichtliche Entwicklung der Nager überhaupt. *Palaeontographica* 31: 19–162.

Schlosser, M. 1902. Beiträge zur Kenntniss der Säugethierreste aus den süddeutschen Bohnerzen. *Geologische und Palaeontologische Abhandlungen Jena* 5 (3): 117–258.

Seemann, I. 1938. Die Insektenfresser, Fledermäuse und Nager aus der obermiocänen Braunkohle von Viehhausen bei Regensburg. *Palaeontographica A* 89: 1–56.

Semyonoff, B.T. 1951. The river beaver in Archangel Province. *In*: *Translation of Russian Game Reports, Vol. 1*, 5–45. Canadian Wildlife Services, Ottawa.

Stefen, C. 1997. *Steneofiber eseri* (Castoridae, Mammalia) von der Westtangente bei Ulm im Vergleich zu anderen Biberpopulationen. *Stuttgarter Beiträge zur Naturkunde, Serie B* 255: 1–78.

Stefen, C. 2001. Barstovian (Miocene) beavers from Stewart Valley, Nevada, and a discussion of the genus *Monosaulax* based on tooth morphology. *PaleoBios* 21: 1–14.

Stefen, C. 2009. The European Tertiary beaver *Chalicomys jaegeri* (Rodentia: Castoridae) revisited. *Kaupia-Darmstädter Beiträge zur Naturgeschichte* 16: 161–174.

Stefen, C. 2011. A brief overview of the evolution of European tertiary beavers. *Baltic Forestry* 17 (1): 148–153.

Stefen, C. 2018. The castorids (Mammalia, Castoridae) from the (early) middle Miocene of Gračanica (Bosnia-Herzegovina). *Palaeobiodiversity and Palaeoenvironments* 100: 301–305.

Stefen, C. and Mörs, T. 2008. The beaver *Anchitheriomys* from the Miocene of central Europe. *Journal of Paleontology* 82: 1009–1020.

Stirton, R.A. 1935. A review of the Tertiary beavers. *University of California Publications in Geological Sciences* 23: 391–458.

Stromer von Reichenbach, E. 1928. Wirbeltiere im obermiocänen Flinz Münchens. *Abhandlungen der Bayerischen Akademie der Wissenschaften, mathematisch-naturwissenschaftliche* 32: 1–74.

Von Meyer, H. 1838. Mittheilungen an Professor Bronn gerichtet, Frankfurt a. M., den 26. Juli 1838. *In*: K.C. Leonhard and H.G. Bronn (eds.), *Neues Jahrbuch für Mineralogie, Geognosie, Geologie und Petrefaktenkunde*, 1838: 413–418.

Von Meyer, H. 1846. Mitteilungen an Prof. Bronn. *Neues Jahrbuch für Mineralogie, Geologie und Paläontologie, Stuttgart* 1846: 462–476.

Von Meyer, H. 1846. Mittheilungen an Professor Bronn gerichtet, Frankfurt a. M., 4. Mai 1846. *In*: K.C. Leonhard and H.G. Bronn (eds.), *Neues Jahrbuch für Mineralogie, Geognosie, Geologie und Petrefakten-Kunde* 1846: 462–476.

Williams, S.A., Prang, T.C., Meyer, M.R., Russo, G.A., and Shapiro, L.J. 2020. Reevaluating bipedalism in *Danuvius*. *Nature* 586: E1–E3.

Żurowski, W. and Kasperczyk, B. 1986. Characteristics of a European beaver population in the Suwalki Lakeland. *Acta Theriologica* 31: 311–325.